August 2014

Doctor's Degree Dissertation

Development of Patch-Type Sensor Module for Energy Expenditure Estimation

Graduate School of Chosun University

Department of IT Fusion Technology

Li Meina

Development of Patch-Type Sensor Module for Energy Expenditure Estimation

에너지 소비량 감지 및 분석을 위한 부착형 센서 모듈

August 25, 2014

Graduate School of Chosun University

Department of IT Fusion Technology

Li Meina

Development of Patch-Type Sensor Module for Energy Expenditure Estimation

Advisor: Prof. Youn Tae Kim

This dissertation is submitted to Chosun University in partial fulfillment of the requirements for a Doctor's degree

August 2014

Graduate School of Chosun University

Department of IT Fusion Technology

Li Meina

This is to certify that the Doctor's dissertation of

Li Meina

has been approved by the Examining Committee for the dissertation requirement for the Doctor's degree in IT Fusion Technology.

Committee Chairperson

Prof. Sung Bum Pan _____ (Sign)

Committee Member

Dr. Myung-Ae Chung _____ (Sign)

Committee Member

Prof. Keun Chang Kwak _____ (Sign)

Committee Member

Prof. Soon-Soo Oh _____ (Sign)

Committee Member

Prof. Youn Tae Kim _____ (Sign)

August 2014

Graduate School of Chosun University

ABSTRACT

Development of Patch-Type Sensor Module for Energy Expenditure Estimation

Li Meina
Advisor: Prof. Youn Tae Kim, Ph.D.
Department of IT Fusion Technology,
Graduate School of Chosun University

For ubiquitous healthcare system, in-situ monitoring of energy expenditure is one of essential requirement. Ubiquitous healthcare means monitoring anyone, in everywhere without any dependence on time and location. Excess nutrient and energy imbalance are considered major important cause of chronic disease. Either of them is base on the individual energy consumption and caloric intake.

In this dissertation, accurate quantification of physical activity energy expenditure has been evaluated by the wireless patch-type sensor module. The patch-type sensor has been designed for real-time monitoring heart rate (HR) and movement index (MI). The major components of the system are the sensor board, the rubber case, and the communication module. The relation test for HR yields an error rate within 2% compared with CASE system (GE, USA). And the correlation coefficient between the average MI and conventionally used agility point score was found to be in the range of 0.8-0.9. The Zigbee telecommunication system was used for communication

over distances of more than 400 m in an open space.

The energy expenditure was estimated by the embedded incremental network. The embedded incremental network includes linear regression (LR) and radial basis function network (RBFN) based on context-based fuzzy c-means (CFCM) clustering. This incremental network is constructed by building a collection of information granules through CFCM that is guided by the distribution of errors of the linear part of the LR model. The results showed significantly high accuracy compared with the conventional network structure (RMSE = 0.78).

요약

에너지 소비량 감지 및 분석을 위한 부착형 센서 모듈

Li Meina
지도교수: 김윤태 교수, Ph. D.
조선대학교 대학원 IT융합학과

유비쿼터스 헬스케어는 시간과 장소에 구애받지 않고 언제 어디서나 사용자의 신체 정보의 모니터링이 가능함을 의미한다. 이 중 에너지 소비량의 실시간 모니터링은 필수 요구 사항 중 하나이다. 과다한 영양분과 에너지 불균형은 고질적인 질병의 원인으로 독립적인 에너지 소비량과 칼로리 섭취량에 기초를 두고 있다.

이 논문에서는 물리적인 활동 에너지 소비량을 무선 부착형 센서 모듈을 이용하여 측정하였다. 패치형 센서는 센서 보드, 고무 케이스, 통신 모듈로 구성되며 실시간 모니터링 심박수 (heart rate)와 움직임 지수(movement index)를 고려하여 설계하였다. 심박수는 CASE 시스템과 비교하여 약 2% 오류율을 보였으며 평균 움직임 지수와 기존의 민첩성 포인트와 비교하여 상관 계수 0.8 ~ 0.9의 범위를 보여주었다. Zigbee 통신 시스템은 개방된 공간에서 400m 이상의 거리에서 통신을 할 수 있다.

에너지 소비는 장착된 incremental network에 의해 측정되며 이는 선형 회귀(linear regression)와 context-based fuzzy c-means(CFCM) 클러스터링을 기반으로 한 방사 기저함수 네트워크(radial basis unction network)를 포함하고 있다. Incremental network는 LR 모델의 선형 부분의 오류 분포로 알려진 CFCM을 통해 정보 미립의 수집을 구성하여 기존의 네트워크 구조와 비교하였을 때 상당히 높은 정확성을 보여주고 있다. (RMSE = 0.78)

Table of Contents

Abstract (English) ····· i
Abstract (Korean) ····· iii
Table of contents ····· iv
List of Tables ····· vii
List of Figures ····· viii
Acronyms ····· x

I. Introduction ····· 1
A. Definition of Energy and Energy Expenditure ····· 1
1. Energy ····· 1
2. Energy Expenditure ····· 1
a) Basal Metabolic Rate (BMR) ····· 2
b) Diet Induced Thermogenesis (DIT) ····· 2
c) Physical Activity (PA) ····· 3
B. Research Necessity ····· 4
C. Methods for Estimating Energy Expenditure ····· 5
1. Direct Calorimetry ····· 5
a) Definition ····· 5
b) Method ····· 6
c) Limitation of Direct Calorimetry ····· 8
2. Indirect Calorimetry ····· 8
a) Definition ····· 8
b) Method ····· 9
c) Limitation of Indirect Calorimetry ····· 10

3. Heart Rate Monitoring ····· 11
a) Definition ····· 11
b) Method ····· 12
c) Limitation of Heart Rate Monitor ····· 12
4. Motion Sensors ····· 13
a) Definition ····· 13
b) Method ····· 13
c) Limitation of Movement Sensors ····· 14
5. Combined Heart Rate and Motion Sensors ····· 14
a) Definition ····· 14
b) Method ····· 15
c) Limitation of Combined Heart Rate and Movement Sensors ····· 16
6. Neural Network for Estimation of Energy Expenditure ····· 17
D. Research Final Target ····· 19
E. Dissertation Organization ····· 20
II. Development of Patch-type Sensor ····· 21
A. System Design ····· 21
1. General System Description ····· 21
2. Heart Rate Monitor Design ····· 24
3. Movement Processing ····· 27
B. Function Test ····· 32
1. Reliability Test ····· 32
2. Performance Evaluation of Heart Rate Detection ····· 35
3. Performance Evaluation of Movement Index ····· 38
4. Field Test Using Bruce Protocol ····· 40
III. Embedded Algorithm ····· 42

A. Incremental RBFN ····· 43
B. RBFN Algorithm ····· 43
C. Context-based Fuzzy C-means (CFCM) Clustering ····· 45
IV. Experiment ····· 48
A. Subjects ····· 48
B. Gas System ····· 48
C. Procedure ····· 50
D. Data Analysis ····· 51
E. Results ····· 52
1. Laboratory Experiment ····· 52
2. Field Test ····· 56
V. Conclusion ····· 60

References ····· 62

List of Publications ····· 70

List of Tables

Table 1.1 Comparison of different methods outcome. ····· 17
Table 2.1 The specification of AirBeat system. ····· 23
Table 2.2. Average maximum adhesive strength on SUS plate and on skin over time. ····· 33
Table 2.3 Average maximum adhesive strength test results after sauna, after shower, and under normal conditions. ····· 35
Table 2.4 Correlation coefficient between the average movement index measured by AirBeat and the conventional agility point score. ····· 39
Table 4.1 Physical characteristics of the subjects (N = 30). ····· 48
Table 4.2 Participants' activity on treadmill base on Bruce Protocol. ····· 51
Table 4.3 RMSE in incremental RBFN model for training data and testing data. ····· 56
Table 4.4 Comparison of the RMSE values for field exercise data. ····· 59

List of Figures

Fig. 1.1 Total energy expenditure. ····· 2
Fig. 1.2 Necessity for measuring human energy expenditure. ····· 5
Fig. 1.3 Direct calorimetry. ····· 7
Fig. 1.4 Indirect calorimetry. ····· 10
Fig. 2.1. Top and bottom views of the patch-type sensor. ····· 22
Fig. 2.2. Photograph of the AirBeat system. ····· 24
Fig. 2.3. Preprocessing for detection of heart rate. ····· 25
Fig. 2.4. Flowchart for heart-rate detection. ····· 26
Fig. 2.5. Flowchart of the movement-index calculation. ····· 28
Fig. 2.6. Procedural diagram of the robust zero-crossing detection algorithm. ····· 29
Fig. 2.7. Theoretical acceleration waveforms with feature points, feature values (triangular areas), and movement index (the sum of areas per second). ····· 31
Fig. 2.8. Peeling test. ····· 33
Fig. 2.9. Comparison of adhesive strength values on SUS plate and on skin. ····· 34
Fig. 2.10. Adhesive strength after sauna, after shower, and under normal conditions. ····· 35
Fig. 2.11. Performance evaluation of the heart-rate detection algorithm. ····· 36
Fig. 2.12. Results of comparison tests of the proposed heart-rate monitor and the reference CASE system. ····· 38

Fig. 2.13. Result of field tests using the Bruce protocol. ····· 40
Fig. 3.1. General flow of the development of the incremental RBFN. ····· 42
Fig. 3.2. Overall flow of processing realized in the design of incremental RBFN. ····· 43
Fig. 4.1 Gas system real-time monitor VO_2 and VCO_2. ····· 49
Fig. 4.2 Gas system real-time monitor energy expenditure. ····· 50
Fig. 4.3 Experiment procedure. ····· 50
Fig. 4.4. Laboratory experiment on the treadmill. ····· 53
Fig. 4.5. Linguistic contexts produced by the error distribution of treadmill data (p = 3). ····· 54
Fig. 4.6. Estimation of cluster centers in each context (p = 3). 55
Fig. 4.7. (a-d) EE prediction performance of incremental CFCM-RBFN. ····· 59

Acronyms

ECG	Electrocardiography
EE	Energy Expenditure
BMR	Basal Metabolic Rate
DIT	Diet Induced Thermogenesis
PPT	Post Prandial Thermogenesis
EI	Energy Intake
TEF	Thermic Effect of Food
PA	Physical Activity
RMR	Rest Metabolic Rate
VO_2	O_2 Consumption
VCO_2	CO_2 Production
HR	Hear Rate
MI	Movement Index
SD	Standard Deviation
BMI	Body Mass Index
MCU	Microprogrammed Control Unit
RBFN	Radia Basis Function Network
CFCM	Context-based Fuzzy C-Means
LR	Linear Regression
RMSE	Root Mean Square Error
LM	Linguistic Model
FFNN	Feed Forward Neural Network

GRNN	Generalized Regression Neural Network
LSE	Lease Squares Estimate

I. Introduction

A. Definition of Energy and Energy Expenditure

1. Energy

Humans oxidise (metabolism) carbohydrate, protein, fat (and alcohol) to produce energy. The energy is needed: To maintain body functions. To breathe, to keep the heart beating, to keep the body warm and all the other functions that keep the body alive. The body warm and all the other functions that keep the body alive. For physical activity, for active movement, muscle contraction. For growth and repair, which require new tissues to be made.

2. Energy Expenditure

The amount of energy used to perform an activity. A baseline of energy is used to maintain life functions.

The energy expenditure (EE) of a man or woman over a whole day is often divided into different components, which can be individually determined [1]. These are (Fig. 1.1):

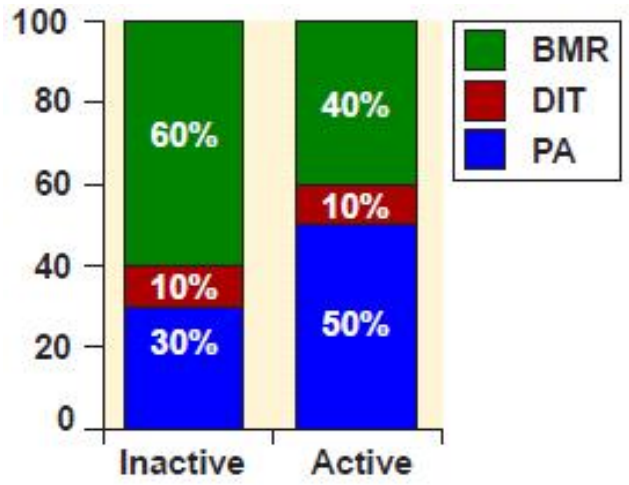

Fig. 1.1 Total energy expenditure.

a) Basal Metabolic Rate (BMR)

The basal metabolic rate is defined as the basal metabolism of an animal. BMR is the minimal rate of energy expenditure compatible with life. In other words, it is the minimum amount of energy (expressed in number of calories) our body needs to stay alive at rest [2]. For the basal metabolic rate estimation to be accurate, several assumptions must be true at the time of measurement: Absence of gross muscular activity. i.e. you must be resting, and your muscles must be relaxed. Post-absorptive state. i.e. 12 hours or more after the last meal. Thermal neutrality. i.e. ambient temperature variations should be minimal (not too hot or cold). Emotional disturbance must be minimal, as studies have shown that emotional upset, particularly apprehension, may result in rises in BMR of from 15-40 percent awake state, as sleep tends to depress BMR by approximately 10 percent.

b) Diet Induced Thermogenesis (DIT)

Also called post-prandial thermogenesis (PPT) or the thermic effect of food (TEF). DIT accounts for about 10% of total energy intake (EI) for a mixed western diet. This is the amount of energy utilized in the digestion, absorption and transportation of nutrients.

c) Physical Activity (PA)

PA is the most variable component of EE in humans. It includes the additional EE above RMR and TEF due to muscular activity and comprises minor physical movement (such as shivering and fidgeting) as well as purposeful gross muscular work or physical exercise. In this study, we focus on the physical activity measurement. The three primary source of energy for human body as follows:

Glucose: $C_6H_{12}O_6 + 6O_2 \rightarrow 6CO_2 + 6H_2O$ (1.1)

Fats: $C_{16}H_{32}O_2 + 23O_2 \rightarrow 16CO_2 + 16H_2O$ (1.2)

Proteins: $C_{72}H_{112}N_2O_{22}S + 77O_2 \rightarrow 63CO_2 + 38H_2O + SO_3 + 9CO(NH_2)_2$ (1.3)

From the equation, we can measure the oxygen consumption or dioxide oxygen production for indirectly estimating energy expenditure. To convert the amount of oxygen consumed into heat equivalents, one must know the type of energy substrate that is being metabolized, that is, carbohydrate or fat, since protein rarely participates in energy metabolism. The energy liberated when fat is the only substrate being oxidized is 4.7 kcal or 19.7 kJ per liter of oxygen used. However, the energy released when carbohydrate is the only fuel being oxidized is 5.05 kcal or 21.1 kJ per

liter of oxygen used. Another measure often implemented, although it is less accurate, estimates the energy expenditure of exercise on the basis of 5 kcal or 21 kJ per liter of oxygen used. Therefore, a person exercising at an oxygen consumption of 2.0 L · min^{-1} would expend approximately 10 kcal or 42 kJ of energy per minute. Consequently, the use of an energy equivalent of 4.825 kcal per liter of oxygen has been suggested for circumstances such as resting or steady-state exercise at mild intensities.

B. Research Necessity

Recently, the rate of chronic disease such as obesity, hypertension, and diabetic is rapidly increased. Excess nutrient and energy imbalance are considered major important cause of chronic disease. Either of them is base on the individual energy consumption and caloric intake. Energy is needed to power muscular activity but that excessive energy storage can lead to obesity and other metabolic disorders, it is important to understand what energy transformation is all about, how energy expenditure can be assessed and quantified, and what strategies either can augment energy provision to enhance performance or can maximize energy utilization to facilitate weight loss or maintain optimal body weight. Simply explained as the following Fig. 1.2.

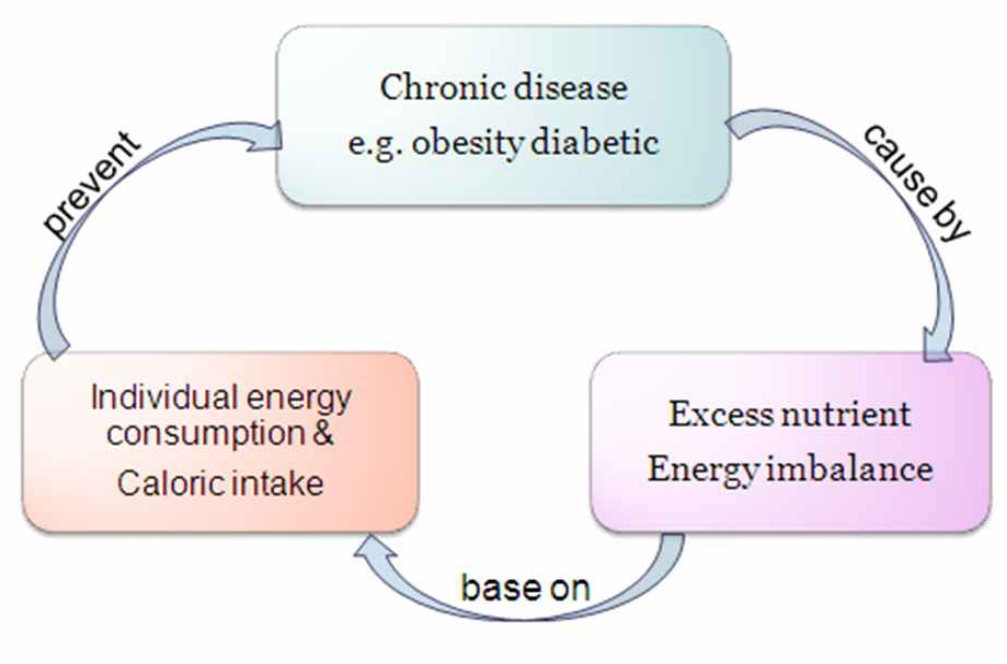

Fig. 1.2 Necessity for measuring human energy expenditure.

C. Methods for Estimating Energy Expenditure

A range of methods are used in the assessment of energy expenditure. These major methods maybe be classified in to direct calorimetry, indirect calorimetry, heart rate monitoring, movement sensors, and combined heart rate and movement sensors. This chapter lists the methods with their advantage and problems.

1. Direct Calorimetry

a) Definition

The process of measuring heat production occurred via both cellular respiration and cell work in an animal is called direct calorimetry.

b) Method

Using a thermally-isolated chamber, the heat subjects dissipated by evaporation, radiation, conduction and convection is recorded accurately and measured precisely. In direct calorimetry, on the other hand, CO_2 production and O_2 consumption are measured [3]. Assuming that all the oxygen is used to oxidize degradable fuels and all the CO_2 there by evolved is recovered, it is possible to calculate the total amount of energy produced.

To measure this heat, a person is placed in a specially designed, insulated chamber (called a calorimeter) supplied with air and surrounded by a jacket of circulating water; the heat production (or energy expenditure) is estimated from changes in the temperature of the surrounding water (Fig. 1.3).

$$Q = cm\Delta T \qquad (1.4)$$

Where Q is the heat energy put into or taken out of the substance, m is the mass of the substance, c is the specific heat capacity, and ΔT is the change in temperature [4].

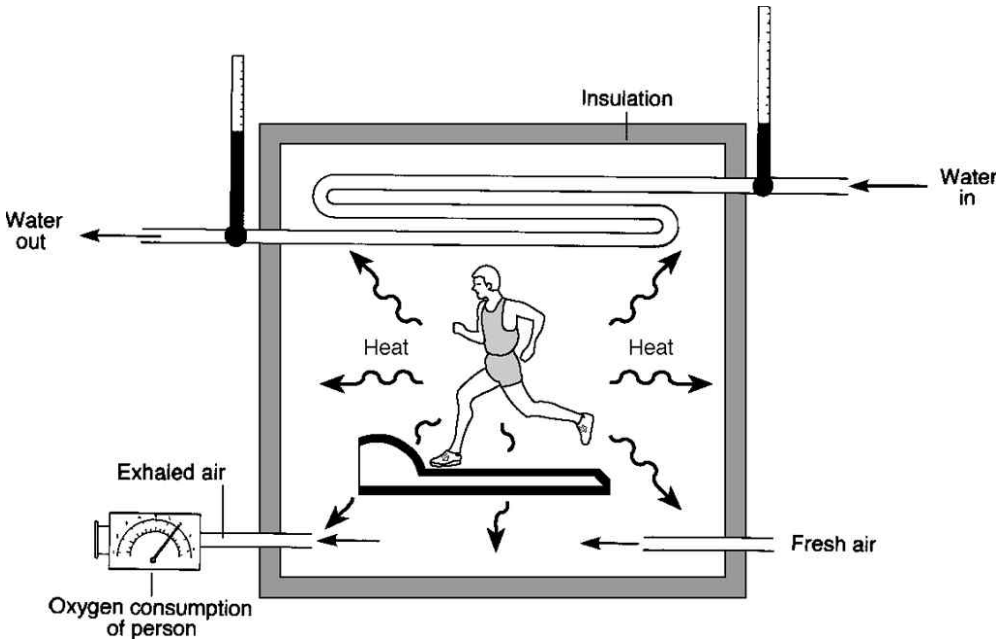

Fig. 1.3 Direct calorimetry.

All calorimeters consist of the calorimeter proper and a jacket or a bath, which is used to control the temperature of the calorimeter and the rate of heat leak to the environment. For temperatures not too far removed from room temperature, the jacket or bath contains liquid at a controlled temperature. For measurements at extreme temperatures, the jacket usually consists of a metal block containing a heater to control the temperature. With nonisothermal calorimeters, where the jacket is kept at a constant temperature, there will be some heat leak to the jacket when the temperature of the calorimeter changes. It is necessary to correct the temperature change observed to the value it would have been if there were no leak. This is achieved by measuring the temperature of the calorimeter for a time period both before and after the process and applying Newton's law of cooling. This correction can be avoided by using the technique of adiabatic calorimetry, where the temperature of the jacket is kept equal to

the temperature of the calorimeter as a change occurs. This technique requires more elaborate temperature control, and its primary use is for accurate heat capacity measurements at low temperatures.

In calorimetric experiments it is necessary to measure temperature differences accurately; in some cases the temperature itself must be accurately known. Modern calorimeters use resistance thermometers to measure both temperatures and temperature differences, while thermocouples or thermistors are used to measure smaller temperature differences.

c) Limitation of Direct Calorimetry

The limitations of direct calorimetry are the expensive of the construction of suitable chamber. Experiment is done by chamber or calorimetry, the subjects are restricted their activity, since change their usual activity patterns. And the fact that such investigations must be made in the laboratory. This is not applicable to measure in free-living conditions. Direct calorimetry is the only method by which continuous recording of energy expenditure for a long time can be obtained. It should consider the investigator time.

2. Indirect Calorimetry

a) Definition

The measurement of the amount of heat generated in an oxidation reaction by determining the intake or consumption of oxygen or by measuring the amount of carbon dioxide or nitrogen released and

translating these quantities into a heat equivalent.

The term 'indirect' refers to the fact that energy production is determined by measuring O_2 consumption and CO_2 production rather than directly measuring heat transfer (direct calorimetry). It is less expensive than direct calorimetry. Its disadvantages are primarily that it remains an expansive technique and requires the use of a hood or a mask that the subject may find confining.

b) Method

There are tow main indirect calorimetry systems for the measurement of VO_2 and hence EE.

Firstly, the 'closed-circuit' method requiring subjects to be isolated from the outside air works well for measuring resting or basal metabolic rate (Fig. 1.4a) [5]. The subject breathes air from the atmosphere. The composition of the air flowing in and out of the lungs is measured to estimate oxygen consumption [6].

Secondly the 'open-circuit' method is more suited to measure exercise metabolism. In this method, airflow and percentage of oxygen and CO_2 are measured precisely to calculate VO_2 and CO_2 consumption (VO_2) and hence respiratory exchange ratio. This method is particularly useful for long-term measurements with subjects at rest or performing only light exercise (Fig. 1.4b). The subject inhales via a face mask from a container filled with oxygen. Expired air goes back to the container via soda lime, which absorbs carbon dioxide. Changes in the volume of oxygen in the container are recorded as the volume of oxygen consumed.

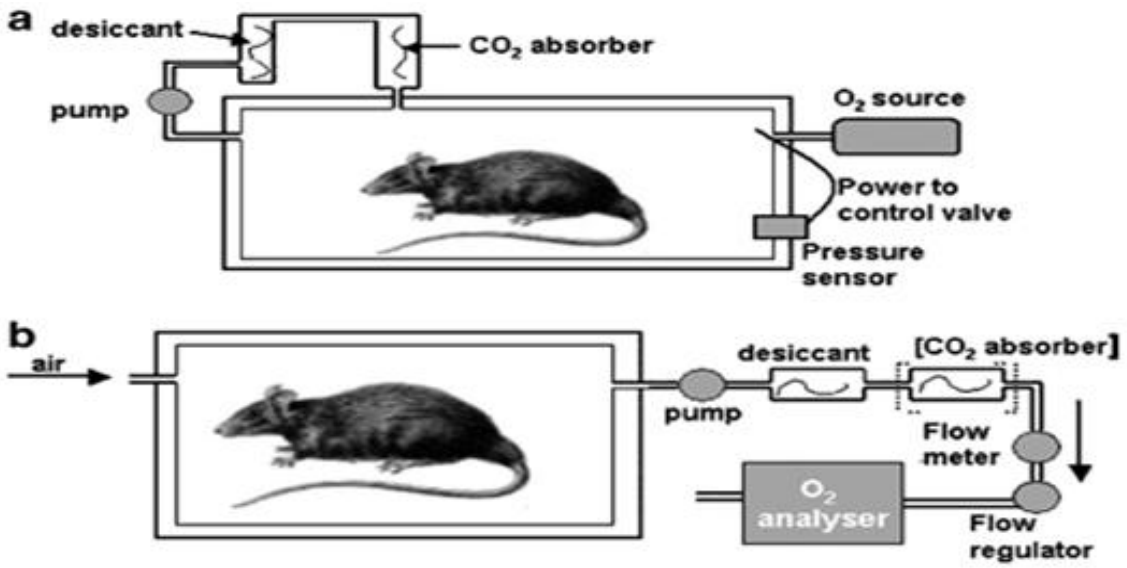

Fig. 1.4 Indirect calorimetry.

a. Closed-circuit indirect calorimetry.

b. Opened-circuit indirect calorimetry.

c) Limitation of Indirect Calorimetry

Indirect calorimetry can be used in the field but continuous recording of activity is difficult. Because this method requires subjects to wear apparatus on face or in mouth, such as ventilated hood system [7].

This method also needs expensive and sophisticated equipment. For example, oxygen consumption measurements often suffered due to the response time of oxygen analyzer [8], this issue related to the sensitivity of oxygen analyzer.

This method can only be accurately used for measuring resting or basal metabolic rate and light exercise during steady state exercise. Steady state conditions are necessary to accurately predict cellular metabolism

through measurements of gas exchange in the airways. If a patients has rapid change in minutes ventilation during a study (hyper or hypoventilation), the measured carbon dioxide at the airway will not accurately reflect cellular levels of carbon dioxide. Thus VO_2 will be artificially higher when the patient hyperventilates and lower during periods of hypoventilation [9]. This is a common problem during mechanical ventilation, especially when a mode that allows of spontaneous ventilation is used.

And this method need consider the consider the system leak problem, especially during mechanical ventilation, area common problem. Failure to capture all of the exhaled volume into the metabolic computer will result in measurement errors. Care should be taken to ensure a tight seal around all circuit fittings as on the artificial airway cuff.

3. Heart Rate Monitoring

a) Definition

Generally, there was a fairly close and linear relationship between HR and EE or VO_2 during steady exercise [10]. This technique has also been validated against electrocardiography (ECG) monitoring. To date, HR is non-invasive, low cost and easy to measure. EE is easily accessible from HR data. HR-based EE-estimates are relatively accurate in steady exercise conditions [11].

However, there are still some limitations. HR does not increase as steeply for a given change in EE, probably due to changes in stroke volume between lying, sitting and standing [12]. For example, HR can vary due to emotional stress, which would result in disproportional rise in HR

for a constant VO_2. At a low level of activities estimations of EE from HR may have errors of up to 30% in individuals, although the average for a group of individuals is likely to be within 10% of the true value.

b) Method

Spurr et al., (1988) developed one method that involves the determination of FlexHR [13]. With this method, an individual's resting metabolic rate (RMR) and HR-VO_2 curve across exercise of varying intensities are first determined. The FlexHR is then calculates as the mean of the highest HR achieved at rest and the lowest HR achieved during exercise. If a given HR observed during field activity is below the FlexHR, then energy expenditure is determined based on RMR. If a given HR is above FlexHR, then energy expenditure is determined based on the individual's HR-VO_2 curve [14]. Even though this method takes into account individual variability in the slope of the HR-VO_2 relationship, it is time-consuming to establish individualized calibration curves.

c) Limitation of Heart Rate Monitor

Heart rate has in estimates of energy expenditure. It can occur during sedentary and light activities because HR can be elevated due to their factors such as stress, hydration, and environmental factors [15].

In particular, HR are affected by biology [16]. Because subject characteristics such as age, sex, body posture, and fitness level affect the slope and intercept of a linear HR-EE relationship.

This method requires individual laboratory calibration curves for accurate estimates of EE [17].

4. Motion Sensors

a) Definition

Motion sensors are mechanical and electronic device that pick up motion or acceleration of limb or trunk, depending on where the monitor is attached to the body. There are several types of motion sensors that range in complexity and cost from the pedometer to triaxial accelerometer [18]. Among motion sensors, triaxial accelerometers which measure acceleration in the vertical, horizontal and mediolateral plane are the most commonly used. But it is unable to detect certain movements such as cycling and upper body exercise. Some devices failed to detect the increased energetic cost of walking on a steep incline.

Lately, a relatively new, commercially available device for assessing energy expenditure, called SenseWear pro armband (SWA) [19]. It monitors various physiological and movement parameters. These data together with demographic information including gender, age, height, and weight, used to estimate energy expenditure with a generalized algorithm. However, its ability to detect energy expenditure during exercise remains questionable. The SWA can not accurately access EE.

b) Method

A new device for assessing energy expenditure, called the SenseWare armband (SWA), came on the market. The device is worn on the right upper arm over the triceps muscle, It has an ergonomic design and can be easily slipped on and off, and it does not interfere with day-to-day

acidities or sleeping [20]. The device has multiples sensors that can measure various physiological and movement parameters simultaneously, including body surface temperature, skin vasodilatation and rate of heat dispassion, as well as a two-axis accelerometer. Data on these parameters, together with demographic information including gender, age, height, and weight, are used to estimate energy expenditure with generalized algorithm, the principal difference between this system and the devices discussed previously is the inclusion of a heat flux sensor [21]. This allows the system to detect a change in heat produced as a result of metabolism.

c) Limitation of Movement Sensors

Accelerometers are generally worn on the hip which limits their ability to detect certain movements such as in weight lifting, cycling, and upper body exercise [22].

There are also unable to discriminate walking or running performed on soft or graded terrain.

5. Combined Heart Rate and Motion Sensors

a) Definition

HR monitoring and accelerometers combined methods are most often chosen for assessing physical activity and energy expenditure. However, there are limitations associated with each method when used alone. The HR monitoring is primarily due to biological variance. HR found to be affected by age, gender and psychological stress [23]. That means it is not possible to differentiate between increases in heart rate due to activity or those due

to stress. On the other hand, the limitations of movement sensors, when used alone, they cannot quantitatively estimate all physical activities, as mentioned before, such as cycling and rowing. The technique is generally unable to adequately detect increases in energy expenditure. These limitations reduce the usefulness of movement sensors alone as instruments to estimate EE in field studies. As errors associated with the two methods are not inherently related [24].

The researchers have studied the combined heart rate and movement sensors for measuring energy expenditure. In these studies, HR and movement counts were recorded at the same time. The activity data were used to separate the HR data into activity and inactivity, which improved the estimates of EE.

AirBeat system that provide HR and mobility index has developed. Until now, a prediction equation using them has not been made for it. Therefore, a well designed experiment is needed to provide more precise prediction of energy expenditure than similar instruments by combining HR and mobility index.

b) Method

Indirect calorimetry is considered to be a precise technique for the measurement of metabolic rate. The principle of indirect calorimetry can be explained by the following relationship:

$$\underset{\text{(Indirect Calorimetry)}}{\text{Foodstuff} + O_2} \text{ ----------> } \underset{\text{(Direct Calorimetry)}}{\text{Heat} + CO_2 + H_2O} \qquad (1.5)$$

Since a direct relationship exists between O_2 consumed and the amount of

heat produced in the body, measuring O_2 consumption provides an estimate of metabolism. In order to convert the amount of O_2 consumed into heat equivalents, it is necessary to know the type of nutrient (i.e.,carbohydrate, fat, or protein) that was metabolized. The energy liberated when fat is the only food stuff metabolized 4.7 kcal (or 19.7 kJ)/L O_2, while the energy released when only carbohydrates are used is 5.05 kcal (or 21.13kJ)/L O_2. Although it is not exact, the caloric expenditure of exercise is open estimated to be approximately 5 kcal (or 21kJ) per liter of O_2 consumed.

The open-circuit spirometry is used to measure oxygen consumption. The volume of air inspired is measured with a device that is capable of measuring gas volumes. The expired gas from the subject is channeled to a small mixing chamber to be analyzed for O_2 and CO_2 content by electronic gas CO_2 in the expired gas is sent to a digital computer by way of a device called an analog-to-digital converter (converts a voltage signal to a digital signal). The computer is programmed to perform the necessary calculations of volume of O_2 consumed per min and the volume of carbon dioxide produced.

In short, the energy expenditure during exercise is estimated by measuring VO_2 (liter per min) using open-circuit spirometry, and then converting it to kcal in following way:

$$EE(kcal/min) = VO_2 \times \text{Energy cost of Oxygen (about 5 kcal/liter)} \quad (1.6)$$

c) Limitation of Combined Heart Rate and Movement Sensors

This method requires HR-VO_2 equations to be developed on each individual for both leg and arm work [25]. This method should consider if multiple sensors are used. The subjects wear cumbersome fitting, which

can affect the accuracy of energy expenditure estimation [26]. In addition, the data analysis is time consuming, thus limiting its use to studies involving small samples [27]. The following Table 2.1 gives a summary of these methods.

Table 1.1 Comparison of different methods outcome.

Method	Measurement	Outcome
Room Calorimetry	CO_2 and VO_2	EE
Indirect Calorimetry	CO_2 and VO_2	EE
Movement Sensors	Acceleration (i.e. body movement)	Counts
HR Monitoring	HR	EE

6. Neural Network for Estimation of Energy Expenditure

Another approach to improve the accuracy is to use the machine learning. Dong [28] uses wearable multi-sensors to extract features of different activities for the construction of the artificial neural network and linear regression. In [29], the authors presented three regression techniques - least squares regression, Bayesian linear regression and Gaussian process regression with the data from treadmill walking using hip-worn inertial sensors. The results show the nonlinear methods have better prediction accuracy. Wang [30] presents a portable-accelerometer and electrocardiogram sensor system with a machine learning-based model for energy expenditure. Lin [31] estimated daily energy expenditure by a

wearable sensor module with a neural network based activity classification algorithm. They employed forward and backward search strategies for feature selection. Radial Basis Function Network (RBFN) and Generalized Regression Neural Network (GRNN) models were employed as energy expenditure estimation. Wong [32] have developed and tested a portable device that measures energy expenditure per unit time of a human subject. Wixted [33] has analyzed the variance of accelerometer-count based energy estimates and identified mechanical, biomechanical, and anthropometrical influences. There are numerous portable instrumentations to measure movement [34-36]. Various methods have demonstrated success in classification or prediction applications [37-42]. Oliver [38] has investigated the utility of a variety of active accelerometer count thresholds for classifying sitting time in a sample of office workers. Xiao [39] has designed a prediction model using the feedforward neural network (FFNN) to reflect the effects of physical activities on the heart rate. In [40], a multi-step HR prediction method is proposed. The HR prediction problem was converted into an initial-value problem for ordinary differential equations. Then the Adams-Bashforth method was used to implement a multi-step prediction. Yuchi [41] and Xiao [42] proposed the well-known FFNN as the predictor model based on the relationship between heart rate and physical activity. The FFNN experimental results showed the potential of the predictor with the results close to the actual data. Vathsangam [43] estimated energy expenditure during treadmill walking using a single hip-mounted inertial sensor with a triaxial accelerometer and triaxial gyroscope. He performed a comparative analysis of the well-known probabilistic techniques in conjunction with inertial data modeling to predict energy expenditure for steady-state treadmill walking. Nonlinear regression methods showed better prediction accuracy compared to linear methods. Lin

[44] presented a wearable sensor module and two representative neural networks (RBFN, GRNN) for activity classification and prediction. He demonstrated the effectiveness of a wearable sensor module and its neural network-based activity classification algorithm for energy expenditure. The research in the literature mentioned above has been performed based on well-known neural networks [39-42, 44] or statistical methods [43] from numerical data. However, these methods have not been considered to be knowledge representation via fuzzy if-then rules with meaningful linguistic labels. In general, it is frequently advantageous to use several computing techniques synergistically rather than exclusively, resulting in construction of complementary hybrid intelligent systems such as neural-fuzzy computing. The effectiveness of these complementary approaches has been demonstrated [45].

The literature of above mentioned have been performed based on well know regression or neural networks from numerical data. However the core of these methods is also based on built linear models. Due to the various activities, the data set could not always be kept on the line and that can reduce the accuracy of estimation. This is therefore we aim to develop a patch-type sensor with embedded architecture of network that can integrate the non-linear parts as the fully input variables for energy expenditure estimation.

D. Research Final Target

For estimating energy expenditure, already have a range of methods. Researchers used variety of sensors and algorithms to estimate energy expenditure. However the accuracy of estimation is difficult. The high accuracy always depend on laboratory. The cumbersome devices are not

comfortable to wear and also need physician to help. The researchers focus on light weight, small size and high accuracy to estimate the energy expenditure.

In this study, we designed a small size, light weight patch type sensor module (AirBeat System) to realize the basic physical activity energy expenditure estimation on the treadmill. The final target: To associate with multiple sensors into relatively homeogenous, small size, long power duration one. Develop software for a sophisticated in determining energy expenditure and can record data for a long time. Realize accuracy energy expenditure estimation from lab to free-living.

E. Dissertation Organization

Chapter Ⅰ introduces the basic background knowledge and the principle of indirect energy expenditure estimation. Explained why we do this research and what's the final target for this study. Chapter Ⅱ presents the common methods for estimating energy expenditure and discusses the problem and limitation of each method. Chapter Ⅲ describes the sensor design, their function and experimental results. Chapter Ⅳ illustrates the embedded software for estimation of energy expenditure. Chapter Ⅴ demonstrates the experimental results. This study is concluded in the last chapter Ⅵ.

II. Development of Patch-type Sensor

It has been confirmed that precise measurements of heart rate and movement index are possible using the patch-type sensor module designed in this research. The proposed movement index shows a good correlation with the conventional agility test and can be used to evaluate an athlete's exercise state. Changes in heart rate and movement index could be confirmed by changes in exercise intensity through analysis of three-axial acceleration and heart-rate variability. Moreover, dependable real-time communication has been secured for a distance of over 400 m for eight people simultaneously. This research has demonstrated that the proposed sensor can be applied to the efficient training of athletes and to emergency forecasting by in-situ heart-rate monitoring.

A. System Design

1. General System Description

The goal of this research has been to develop the AirBeat as a small patch-type system which can be attached to the subject's chest during exercise. The major components of the system are the sensor board, the rubber case, and the communication module.

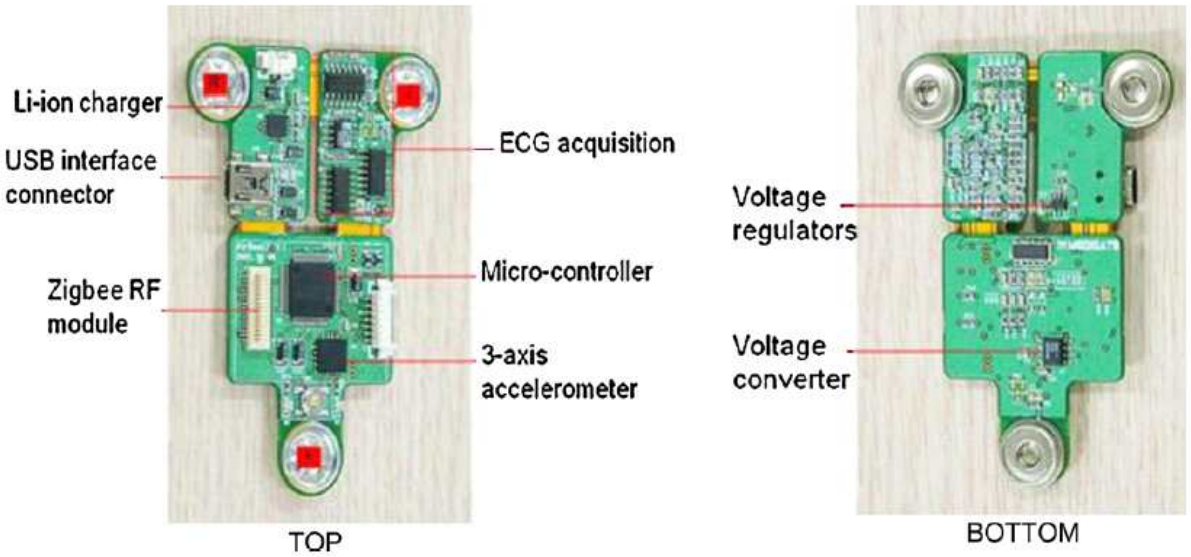

Fig. 2.1. Top and bottom views of the patch-type sensor.

Fig. 2.1 shows a photograph of the sensor chip. As input data, a number of sensor signals were selected, including one-channel ECG and three-axis acceleration [46]. The communication module, ECG sensor, and accelerometer are placed on the top of the sensor, and the switch capacitor voltage converters and regulators are placed on the bottom. The USB interface connector is used for charging the sensor. The signals are interpreted appropriately as heart rate, heat stress, and movement index using a signal-processing algorithm. The microcontroller uses a Texas Instruments MSP 430 chip with 60 KB flash memory, 2048 B SRAM memory, and 8 MHz clock frequency. Table 2.1 lists the specification of AirBeat system.

Table 2.1 The specification of AirBeat system.

Items	Performance
Channel	8ch
Resolution	12bit
Sampling Rate	200/s
Frequency B.W.	1Hz~50Hz
Power	LI-ION
Max HR	250/m
HR Detection Error	Below 10%
Power	3.3V
Comm. Module	ZigBee
Comm. Distance	400 m
MCU	MSP430 (TI,USA)
Electrode	Jumper setting available
Size	6 cm * 9 cm, 20g

Two quasi-triangular flexible PCB boards are combined in the sensor, as shown in Fig. 2.2. The device consists of flexible printed circuit boards which include analog and digital circuitry and onboard sensors. The shape of the FPCB is a quasi-triangle of 60 mm x 80 mm (width, length), and the total system weight is 41 g, including a set of Li-ion rechargeable batteries. The recharger power output is 5V, 3A, and the input power is

220V, 60Hz.

(a)Sensor board.

(b) Silicon packaging case.

Fig. 2.2. Photograph of the AIRBEAT system: (a) sensor board including battery and Zigbee module; (b) silicon packaging case, 85mm×110mm×1.6mm.

2. Heart Rate Monitor Design

For ECG measurement on the chest, three electrodes are used for a single channel. Three dry Ag/AgCl electrodes without gel are mounted on a conductive adhesive patch. The ECG analog circuitry was specifically designed for effective motion artifact rejection during exercise. The input data were then filtered and amplified, as shown in Fig. 2.3. This part of the device consists of an instrumentation amplifier, a notch filter, and a non-inverting amplifier with a total gain of 80 dB and a bandwidth of 40Hz. To monitor exercise, it is not necessary to measure the perfect QRS because during exercise, much noise will be generated. The trigger signal can also provide the HR information.

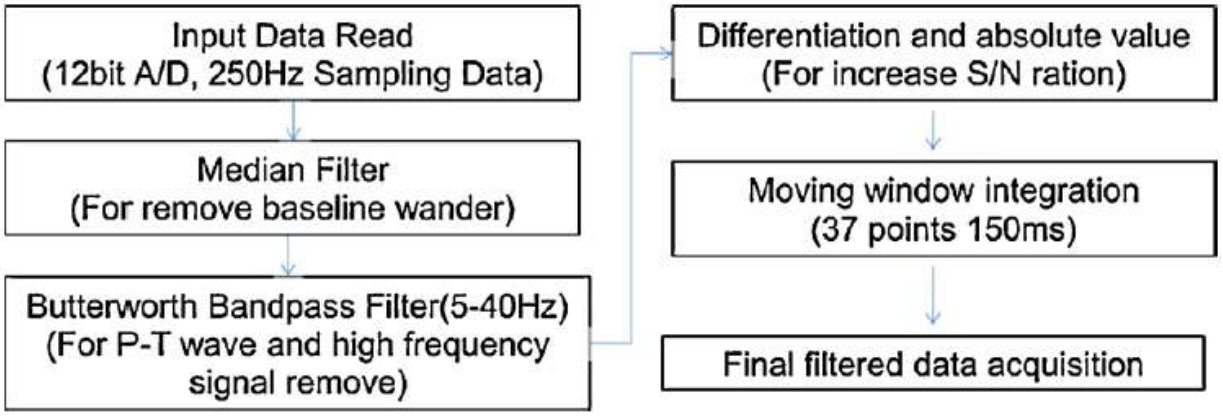

Fig. 2.3. Preprocessing for detection of heart rate.

The ECG signal is then converted into a digital signal with a sampling rate of 200 Hz for heart-rate estimation. The heart-rate detection algorithm is used to analyze the athlete's heart rhythm during exercise. A well-known bandpass-filter-based R-wave detection algorithm has been redesigned to make it more robust during motion. After digital conversion of the ECG signal using a 200-Hz sampling rate, the data undergo preprocessing, including band pass filtering, differentiation, squaring, and calculation of a moving average. Then QRS complexes with positive peak values are detected using an adaptive threshold technique.

The detected QRS peaks are temporarily stored for three seconds. Then a set of motion artifact rejection steps is carried out. First, any QRS peaks which are less than 50% of the previous value are dropped. Second, any QRS complex which does not show a heart-rate value between 30 and 250 is rejected. Finally, if a QRS complex is more than 15 beats longer than the previous value, it is also ignored. This means that the observed heart-rate variation lies within the known range of physiological variation. Next, the algorithm calculates the final heart rate by processing the acquired signal according to the flowchart shown in Fig. 2.4. Performance evaluation of the heart-rate detection procedure was conducted using a

commercial stress ECG monitor (CASE system, GE Medical, USA).

Fig. 2.4. Flowchart for heart-rate detection.

3. Movement Processing

To detect acceleration changes during exercise, a three-axis accelerometer (MMA7260Q) was used. This device is a cheap capacitive micro-machined accelerometer featuring good sensitivity, low power consumption, and very small size. With this sensor, the AirBeat can measure the athlete's motion signals in the range of -6g to 6g and calculate the movement index as proposed in this study.

The authors suggest a movement index as a helpful indicator of exercise performance and a measure of agility. Agility is the ability to change the body's position and requires a combination of balance, coordination, speed, reflexes, and strength.

In the present study, the movement index is calculated using the steps shown in Fig. 2.5. First, the acceleration signal is digitized using a 12-bit analog-to-digital converter with a 100-Hz sampling rate. Then the converted data are preprocessed using band pass filtering and a robust zero-crossing detection algorithm. The zero-crossing detection algorithm extracts characteristic points from the raw data. Using the extracted points, the final movement-index value can be calculated.

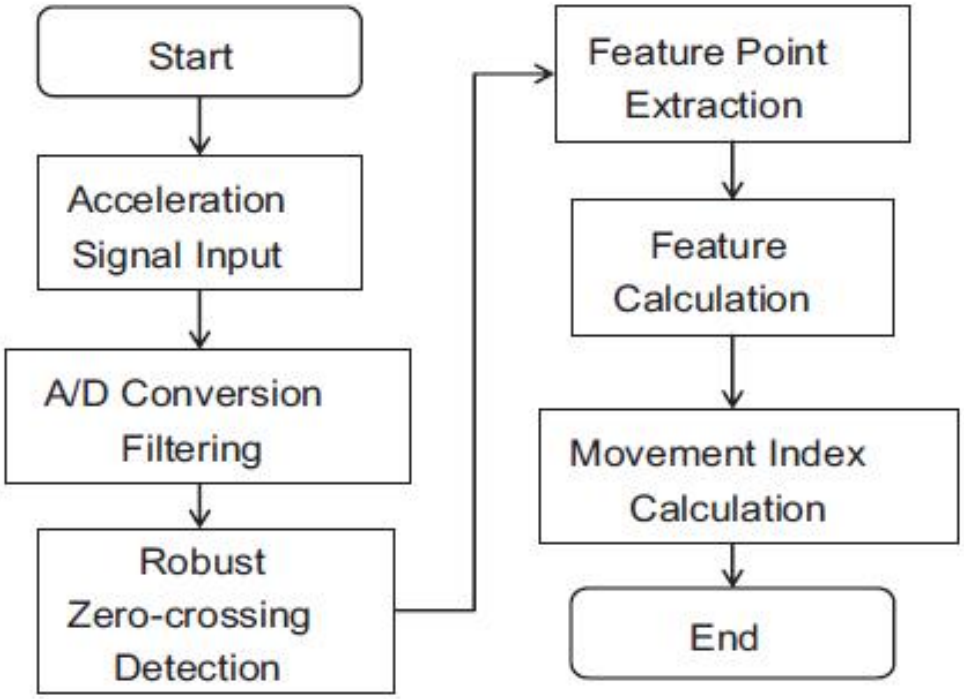

Fig. 2.5. Flowchart of the movement-index calculation.

The zero-crossing detection step described above is the most important step in the algorithm. “Zero crossing” is a commonly used term in electronics, mathematics, and image processing. In mathematics, it usually refers to a change of sign, e.g., from positive to negative, that is, a crossing of the axis (the zero value) in a plot of a particular function. In a real-world acceleration signal, there are many noise factors which create signal artifacts. As a result, a robust zero-crossing detector must be designed.

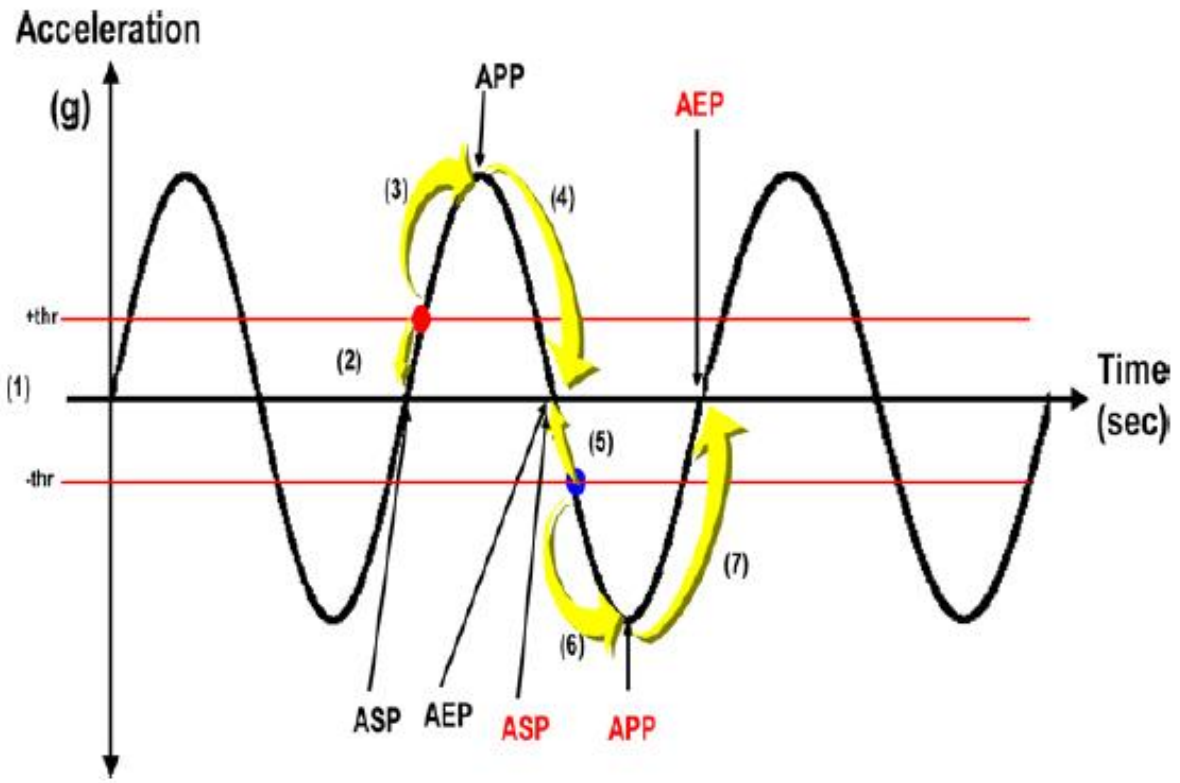

Fig. 2.6. Procedural diagram of the robust zero-crossing detection algorithm.

As shown in Fig. 2.6, the proposed zero-crossing detection algorithm consists of the following steps:

(1) Determine the positive and negative thresholds (+thr and -thr) assuming the noise margin.

(2) When the signal strength becomes greater than +thr, the zero-crossing point can be determined by decreasing the sample index from the intersection point. Then the zero-crossing point is labeled as the ASP (Acceleration Start Point).

(3) Once the ASP has been found, the APP (Acceleration Peak Point) can be detected as a peak value by increasing the sample index from the +thr intersection point.

(4) The zero-crossing point can then be found as the AEP (Acceleration End Point) by increasing the sample index.
(5), (6), (7) Steps (2) through (4) are repeated for the negative threshold, -thr.

This procedure reduces the probability of false-value extraction due to motion artifact noise. An algorithm performance test achieved a 99% detection ratio for a simulated acceleration signal.

Based on the feature points extracted using the robust zero-crossing detection algorithm, feature values can then be calculated. The feature value to be computed was experimentally selected as the triangular area determined by the ASP, APP, and AEP, because the value of this area shows an excellent correlation with agility performance tests in the zigzag run, sidestep test, Burpee test, and shuttle run test. Finally, the movement index can be defined as the average of the triangular areas of the acceleration graph for each second, as shown in Fig. 2.7.

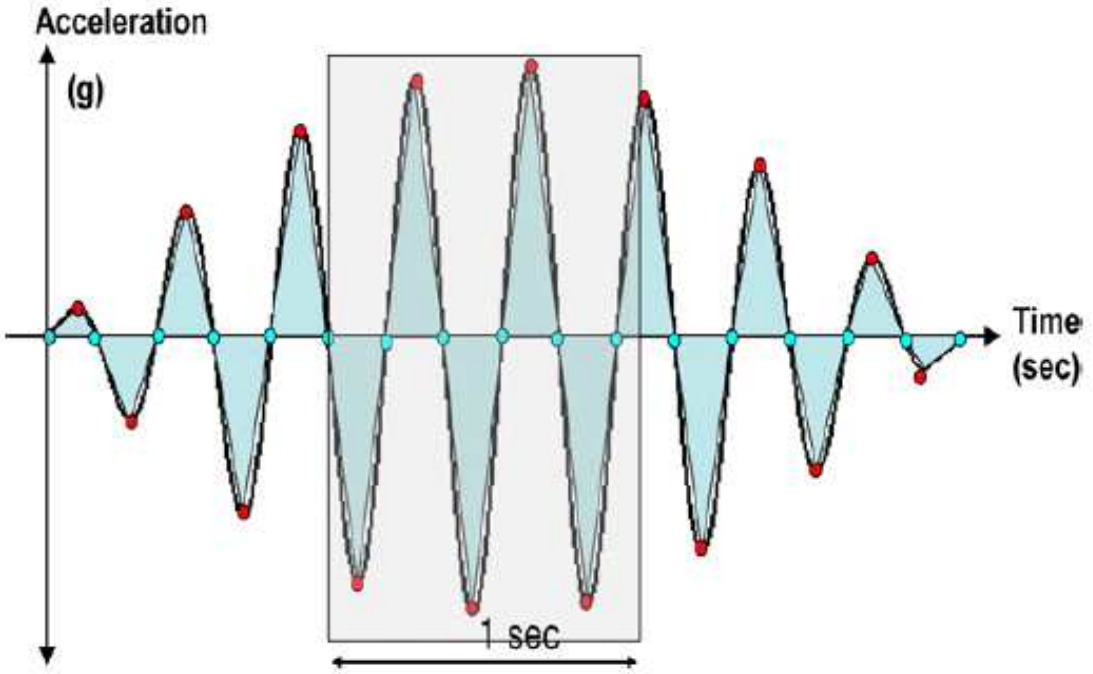

Fig. 2.7. Theoretical acceleration waveforms with feature points, feature values (triangular areas), and movement index (the sum of areas per second).

To enable wireless exercise management, the acquired sensor data should be passed to a central monitoring station. In the AirBeat, a commercial Zigbee telecommunication module [47] is used for data transfer. This module (LM2400) features good data communication range (over 400 m in an open space) without data loss. It operates in the 2.4-GHz ISM (Industrial, Scientific and Medical) band and contains an embedded 8051-compatible microcontroller. The portable transmitter includes 3.3V Li-ion rechargeable batteries with a continuous operation period of approximately two hours. Moreover, it comes with a certified software package and supports the 802.15.4 MAC (Media Access Control) protocol. In practical application, the AirBeat uses a flexible printed circuit board, silicone rubber packaging, and a silicone rubber adhesive. Thanks to the

FPCB (Flexible Printed Circuit Board) and silicone rubber packaging, the whole system is flexible and can be attached to the user's chest. The silicone rubber adhesive can be washed and reused repeatedly. Dow Corning 7-9800 is used as a soft-skin adhesive.

B. Function Test

1. Reliability Test

When monitoring athletes' training, electrodes without gel materials are usually difficult to stick firmly onto the chest. The contact area between the electrodes and the skin may easily slip and release during athletic activities. This factor always affects the ECG signal and produces noise signals. In addition, the ECG signal is easily interfered with by the moisture and electrical resistance of human skin. To address this problem, the authors have tested the reliability of the patch-type sensor.

The soft-skin adhesive coating is made of a non-woven spunlace fabric [48] which features good ventilation, water penetration, and temperature resistance (-73°C to 75°C). The purpose of this part of the study is to test the adhesive strength of the three-point ECG electrode. The coating was patched onto an SUS plate and also onto skin. After some time, the top of the coating was fixed onto a hook and then connected to a push-pull gauge (Fig. 3.8) and pulled down at a speed of 10 mm/sec. The push-pull gauge measured the maximum force applied to the coating before it peeled off. The test was repeated five times.

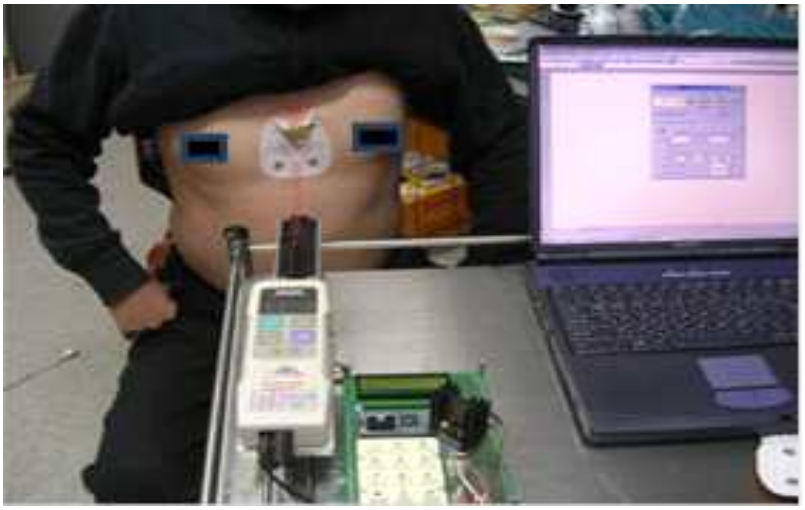

Fig. 2.8. Peeling test.

The results of the peeling test are shown in Table 2.2. When the coating was initially patched onto the SUS plate and onto skin, the results showed that the SUS plate is more adhesive than skin. However, the skin adhesive bond became stronger over time. Fig. 2.9 shows the comparison between the adhesive strength on the SUS plate and on skin over time.

Table 2.2 Average maximum adhesive strength on SUS plate and on skin over time.

	SUS plate	Skin (immediately)	Skin (after 10 minutes)	Skin (after 2 hours)
Average Max Adhesive strength	0.401kgf	0.332kgf	0.466kgf	0.658kgf

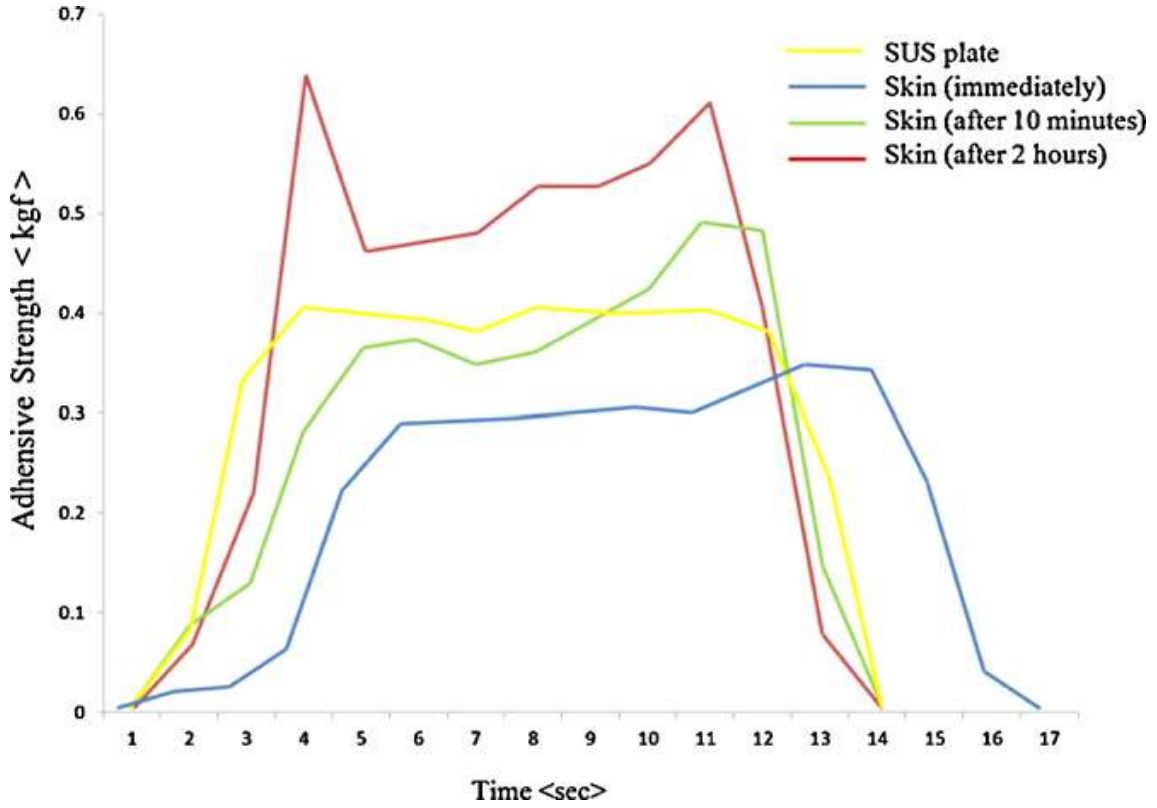

Fig. 2.9. Comparison of adhesive strength values on SUS plate and on skin.

As athletes perform long high-intensity exercise, sweat may make patch sensors drop off. To address this possible drawback, three participants were tested in a sauna and after taking a shower. The first participant was patched for one hour under normal conditions and then in the sauna for another hour. After a one-hour rest, the participant was tested by the pull test. The second participant remained in a normal state for three hours and was then tested by the pull test. The third participant remained under normal conditions for two hours and then took a shower for approximately one hour. The results are shown in Fig. 2.10. Table 2.3 summarizes the average maximum adhesive strengths obtained.

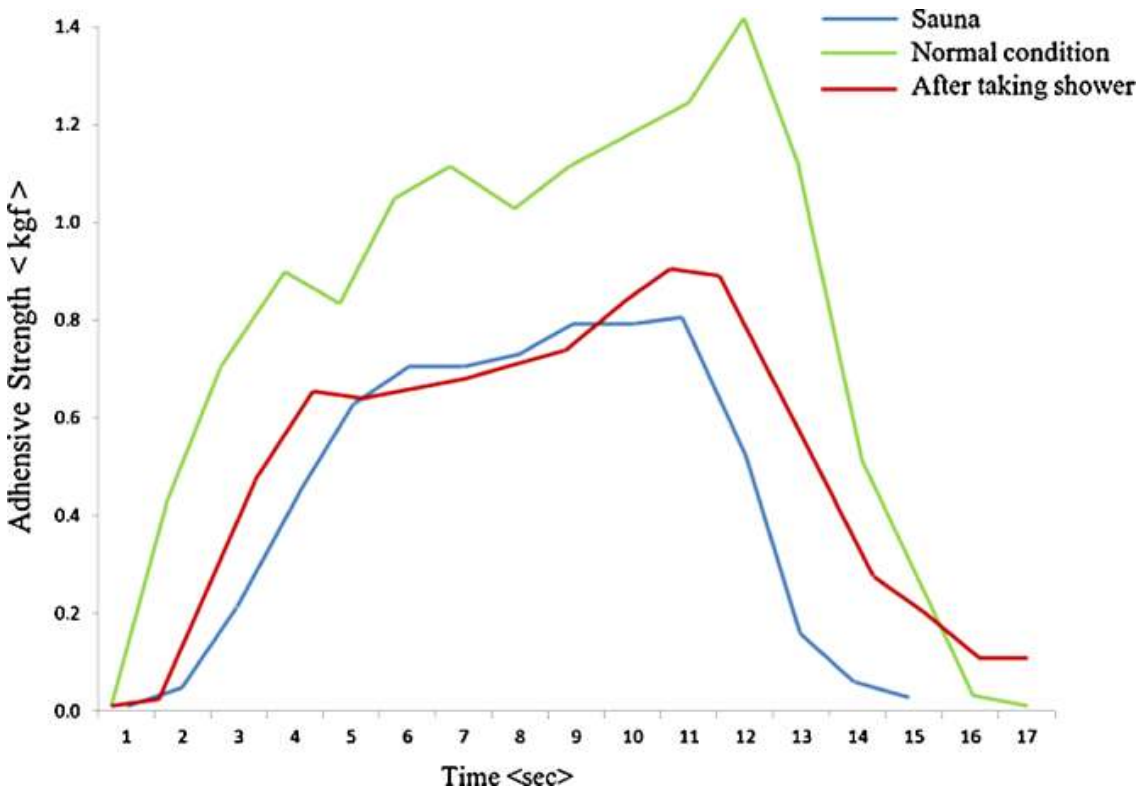

Fig. 2.10. Adhesive strength after sauna, after shower, and under normal conditions.

Table 2.3 Average maximum adhesive strength test results after sauna, after shower, and under normal conditions.

	Sauna	Normal condition	After shower
Average Max Adhesive strength	0.775 kgf	1.387kgf	0.863kgf

2. Performance Evaluation of Heart Rate Detection

Performance evaluation of the heart-rate detection algorithm was conducted by comparing it with the reference system and changing the run speed as shown in Fig. 2.11(a).

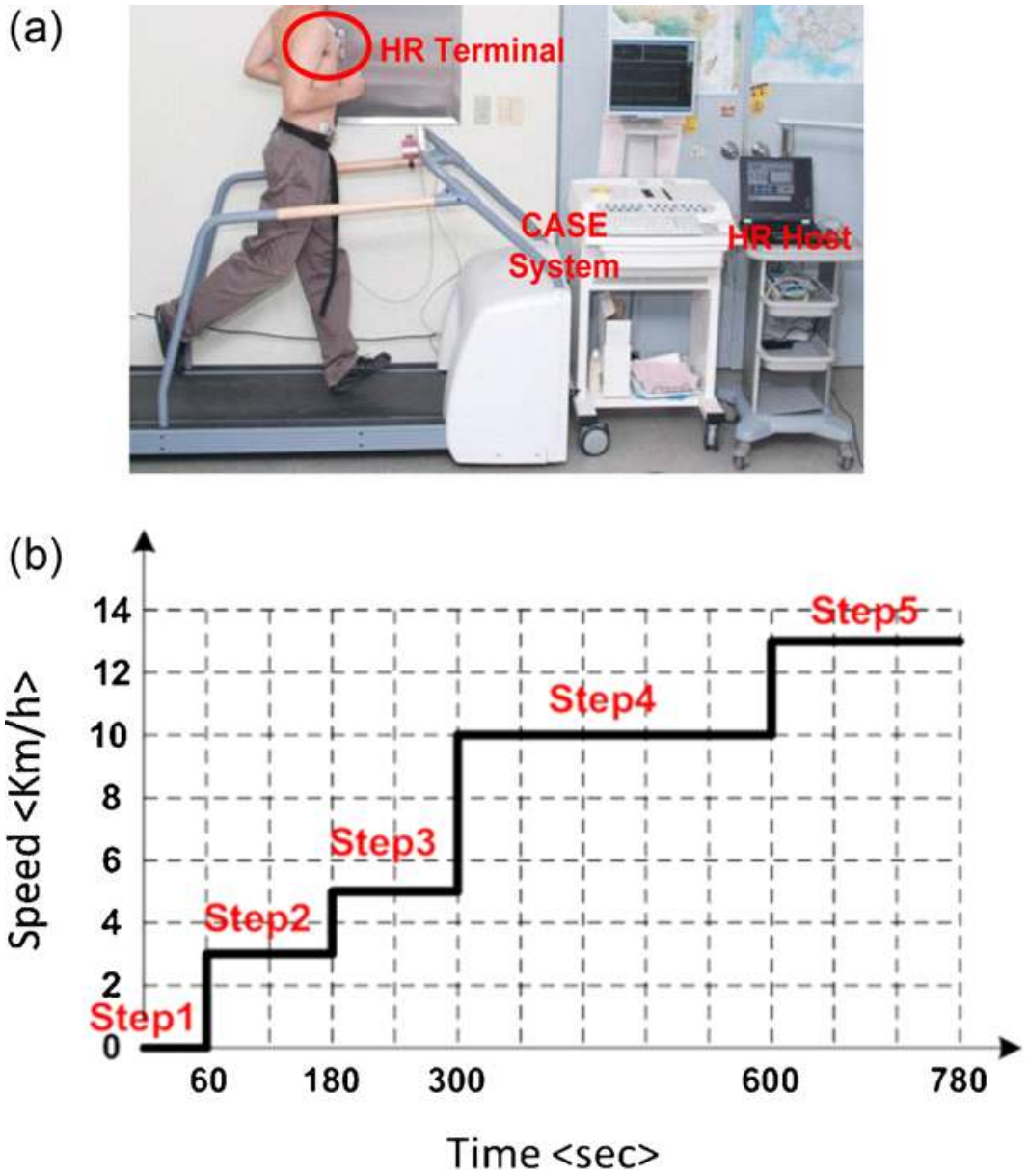

Fig. 2.11. Performance evaluation of the heart-rate detection algorithm: (a) experimental setup; (b) speed profile used in the test.

In this test, a commercial stress ECG monitor (CASE system, GE Medical, USA)[49] was used as the reference system. Heart-rate data were simultaneously gathered from the reference system and from the device designed in this research. The test subjects were people in their twenties. The predetermined speed profile shown in Fig. 2.11(b) was used for exercise load control. The total 13-minute test was divided into five steps with a running speed varying from a minimum of 0 km/h (resting) to a maximum of 13 km/h.

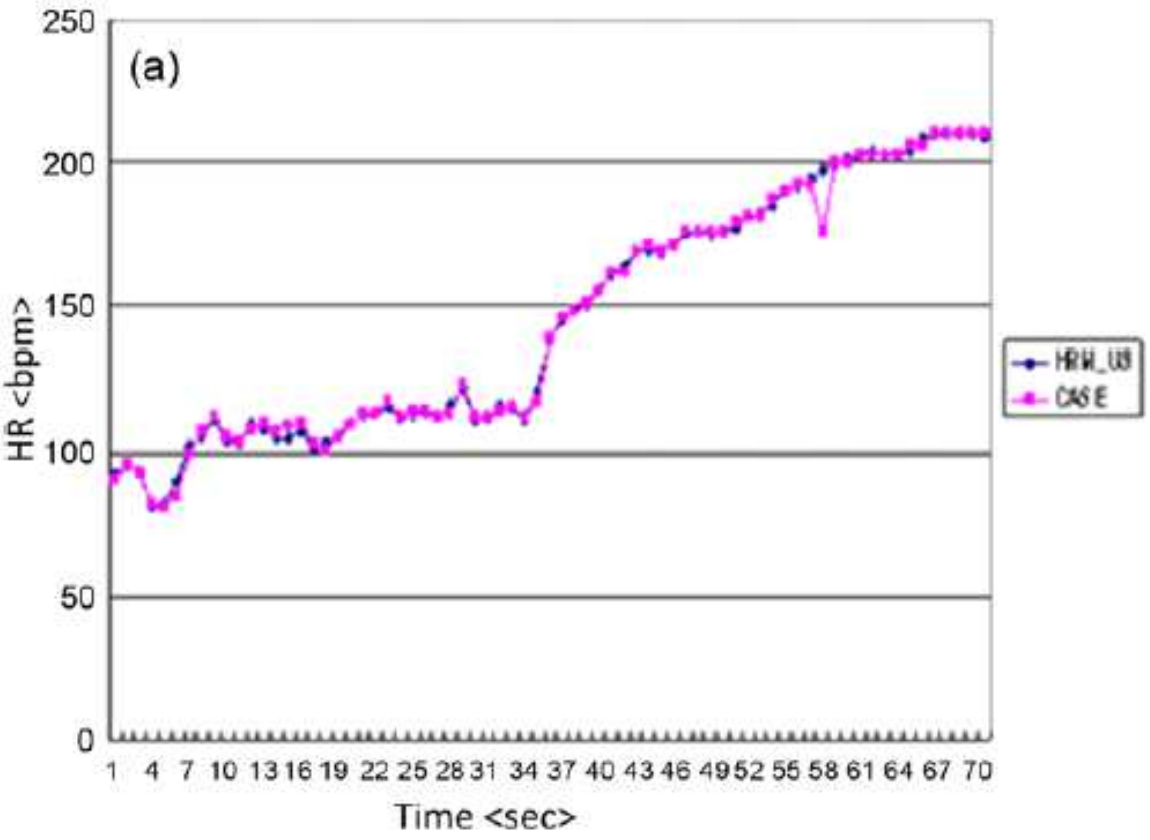

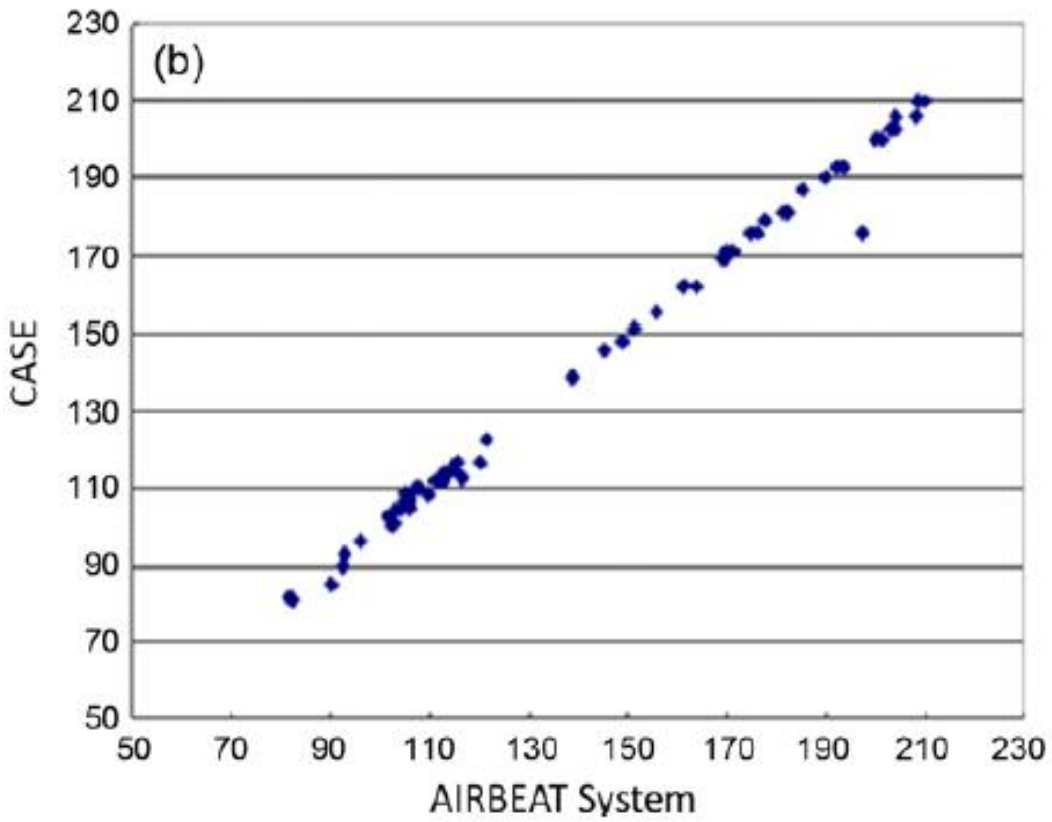

Fig. 2.12. Results of comparison tests of the proposed heart-rate monitor and the reference CASE system: (a) graph of time versus heart rate; (b) graph of heart-rate values from the proposed system (x-axis) versus those from the CASE system (y-axis).

Fig. 2.12 shows the results of comparison tests of the proposed heart-rate monitor and the data from the reference system.

The average heart-rate error between the proposed HR monitor and the CASE system was less than 2%. It is evident that the AirBeat shows good HR detection performance compared with a commercial stress ECG monitor over a wide range of exercise loads.

3. Performance Evaluation of Movement Index

Performance evaluation of the movement index was conducted in two steps. First, the feature-point extraction function was evaluated in a noisy environment using simulated data. For this test, acceleration signals were simulated using a signal generator with noise-level control. Using the robust zero-crossing detector described above [50], the proposed algorithm showed good feature-point extraction characteristics with maximum 1% error.

Second, a comparison test was carried out to evaluate how well the proposed agility index represents the athlete's actual exercise state. Ten subjects performed a zigzag runtest, a 20-mshuttle run [51], a Burpee test [52] and a sidestep test for ten repetitions of each test. These tests are commonly used to evaluate an athlete's performance and to provide a basis for an exercise prescription [53].

Table 2.4 shows the correlation coefficient between the average movement index measured with AirBeat and the conventional agility point score (time or counts which were tested) by a supervisor in each test. The proposed movement index clearly shows a good correlation with the conventional agility test and can be used to evaluate an athlete's exercise state.

Table 2.4 Correlation coefficient between the average movement index measured by AirBeat and the conventional agility point score.

Test	Correlation coefficient
Zigzag run	0.90
Shuttle run	0.80
Burpee test	0.89
Side step test	0.91

4. Field Test Using Bruce Protocol

The field test of the AirBeat as designed was performed according to the Bruce protocol [54]. The Bruce protocol is an exercise protocol with multiple steps where each step is performed for three minutes and exercise intensity is increased in each step.

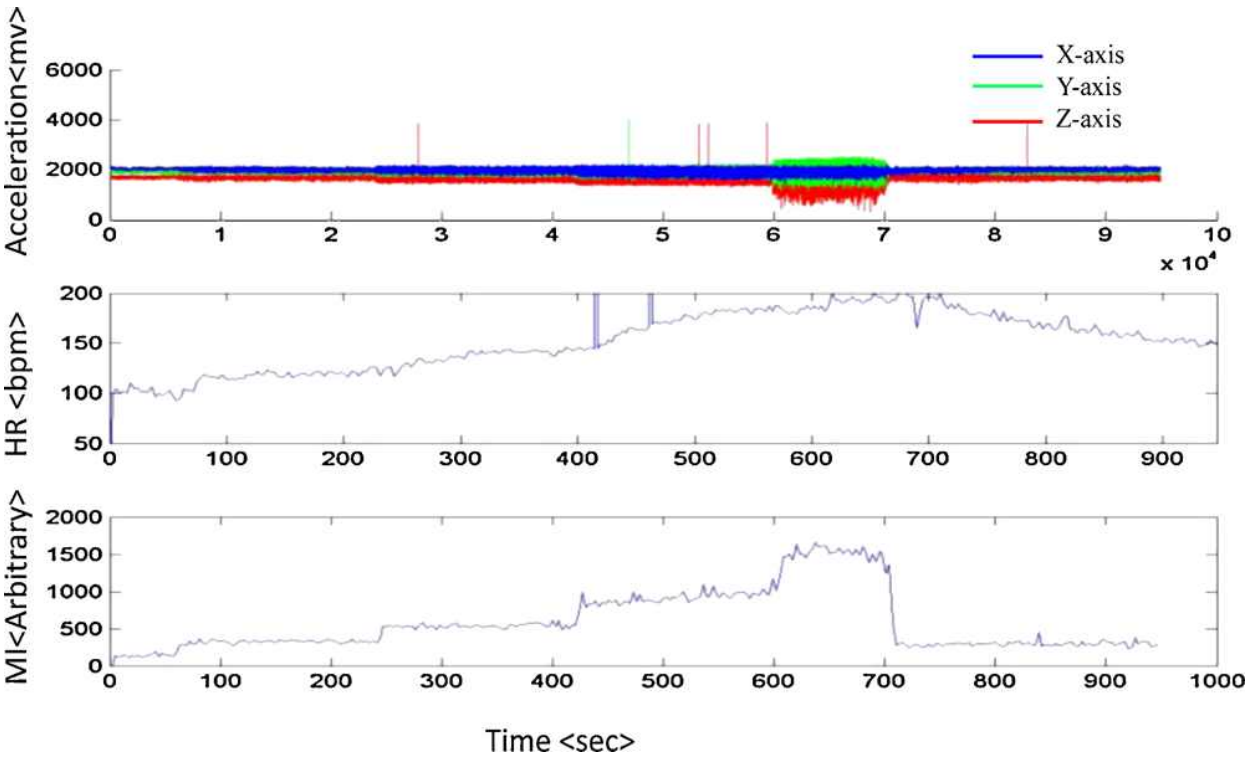

Fig. 2.13. Result of field tests using the Bruce protocol.

Fig. 2.13 shows the result of the field tests using the Bruce protocol. The participants performed exercise ranging from walking to running at different speeds and gradient slopes for 15 minutes on the treadmill. The movement index clearly shows the steps according to the different exercise intensities. The acceleration is shown by three different colors representing

x, y, and z planes. According to the test results, changes in HR and movement index can be reliably monitored and measured during exercise using the proposed device. These results confirm that the AirBeat could be used as an exercise evaluation system for athletes.

III. Embedded Algorithm

An incremental RBFN is proposed in this study; its structure is formed in two steps, as shown in Fig. 3.1. In the first step, we build a standard regression model that can be treated as a preliminary construct capturing the linear part of the data and thus, forming the backbone of the entire construct. Next, all modeling discrepancies are compensated by a collection of receptive fields that become attached to the regions of the input space where the error is localized. The receptive fields are in the subspaces of the original input space rather than in the entire input space. The incremental RBFN is reconstructed by building a collection of information granules formed by using the context-based fuzzy C-means (CFCM), which is guided by the distribution of errors of the linear part of the model. The so-called CFCM is the input space conditioned on the basis of linguistic landmarks. We determine the optimal context of input variables by trial and error in order to realize a high-accuracy output. The principle of the designed architecture can be summarized as follows: adopt a construct of an LR as a first-principle "global" model, and then refine it through a series of "local" receptive fields that capture the remaining and more "localized" non-linearities of the system.

Fig. 3.1. General flow of the development of the incremental RBFN.

A. Incremental RBFN

The main design of the incremental RBFN is shown in Fig. 3.2. The two inputs are placed according to the LR design. The non-linear datasets are formed in a collection of input-error pairs. The input-error pairs are found in the contexts space E and characterized by triangular membership functions. CFCM is completed by the individual fuzzy set of the context in the previous step. The clusters are formed using the RBFN model center values from the hidden layer. Finally, the output layer is summarized by each of hidden layer. The results of incremental RBFN are combined with the linear part and RBFN model output. The numeric bias term is added as the eliminated eventual systematic shift of the results.

Fig. 3.2. Overall flow of processing realized in the design of incremental RBFN.

B. RBFN Algorithm

The RBFN is attractive in that it can be used for functional approximations, localization, interpolation, and cluster modeling [55], which makes it useful in many applications. It has a three-layer structure: an input layer that feeds feature vectors into the network, a hidden layer that calculates the outcome of basic functions, and an output layer that calculates the linear combination of the basic functions. The hidden layer considers a Gaussian basis function centered at v_i with the width parameter σ; therefore, the receptive fields w_i of hidden unit i are calculated as follows:

$$w_i = \exp\left[-\frac{(x - v_i)^2}{2\sigma_i^2}\right] \qquad (3.1)$$

where x denotes a multidimensional input vector; v_i represents the center associated with hidden unit i, and σ denotes the width coefficient. The output of the hidden units is normalized between 0 and 1. The activation level of an output unit is determined as follows:

$$y(\mathrm{x}) = \sum_{i}^{M} g_i w_i \qquad (3.2)$$

where g_i denotes the weight from the hidden unit to output y.

From the above equation, we can know that the network performance is highly dependent on the receptive fields and the connections of the neuron in the output layer of the network. The RBFN is two-layer feed forward network. Further, the network training is divided into two stages: first, the

centers from the input to the hidden layer are determined, and then, the weights are determined from the hidden layer to the output layer. Once we have formed the receptive field, the optimization of weights of the neuron in the output layer becomes straight forward [56, 57]. Since the centers and widths are fixed after they are selected, the RBFN often results in an unsatisfying performance when the input patterns are not particularly clustered. Therefore, the context-based C-means clustering was applied in the input space by ensuring that the resulting reception fields directly associated with the clusters already constructed in the output space for achieving excellent performance.

C. Context-based Fuzzy C-means (CFCM) Clustering

The CFCM algorithm is used for predicting the cluster centers. The context is defined by the error of LR. The given data then belong to the corresponding membership values. The partition matrices induced by the l -th context can be defined as follows:

$$U(W_l) = \left\{ u_{ik} \in [0,1] | \sum_{i=1}^{c} u_{ik} = W_{lk} \forall k \right\} \quad (3.3)$$

where W_{lk} denotes a membership value of the k -th data point implied b y l -th context. The underlying objective function can be expressed in the standard format as follows:

$$Q = \sum_{i=1}^{c} \sum_{k=1}^{N} u_{ik}^{m} \| x_k - v_i \|^2 \quad (3.4)$$

where m denotes a real number greater than 1, u_{ik} represents the degree of membership of x_k in the cluster k, u_{ik} refers to the k-th element of the dimensional measured data, x_k denotes the v_i dimension center of the cluster, and || · || stands for a distance function between any measured data and the i-th center cluster. The minimization of objective function is realized by iteratively updating the values of the partition matrix and the prototypes as shown above. The update of the partition matrix u_{tik} and the cluster center v_i is computed as follows:

$$u_{tik} = \frac{w_{tk}}{\sum_{j=1}^{c} \left(\frac{\| x_k - v_i \|}{\| x_k - v_j \|} \right)^{\frac{2}{m-1}}} \qquad (3.5)$$

$$i = 1, 2, \cdots, c; \quad = 1, 2, \cdots, N$$

where j denotes the iteration step and u_{tik} represents the element of the membership matrix induced by the i -th cluster and the k -th data element in the t -th context.

$$v_i = \frac{\sum_{k=1}^{N} u_{tik}^{m} x_k}{\sum_{k=1}^{N} u_{tik}^{m}} \qquad (3.6)$$

The proposed algorithm is composed of the following steps:

Step 1: Divide the error pairs into contexts by average distribution.

Step 2: Normalize matrix U with random values between 0 and 1 such that Equation (3.1) is satisfied.

Step 3: Calculate the context-based cluster v_i , using Equation(3.6).

Step 4: Compute the cost function according to Equation (3.3). Stop if either it is less than the low bound or its improvement over the previous iteration is less than a certain threshold.
Step 5: Compute a new U and update using Equation (3.5). Go to step 4.

The training procedure for the RBFN consists of two major phases: unsupervised and supervised learning. In the unsupervised phase, the number of receptive fields is defined, and then, the CFCM algorithm is used for determining the center and spread of the receptive field. In the supervised phase, the weight between the output of the RBFN and the receptive fields is computed using the least squares estimate (LSE), which is possible because of a linear relationship with respect to the parameters to be estimated. Further, the RBFN employs optimization techniques with learning rules to fine-tune its parameters to match a dataset produced by a target system to be modeled. Because such a dataset always contains the desired outputs to be reproduced by the network, the underlying learning rule is referred to as supervised.

IV. Experiment

A. Subjects

Thirty students from Chosun University (Table 4.1) were participated in gradual exercise test on the treadmill for estimating caloric expenditure in accordance with the Bruce protocol. The whole process from walking to running total 12 minutes. The outdoor exercise were performed four activities from walking to running.

Table 4.1 Physical characteristics of the subjects (N = 30).

Variable	Men (N = 17)		Women (N = 13)	
	Mean	Range	Mean	Range
Age, year	26 ± 2.1	24~27	25.8 ± 3.2	23~28
Height, cm	169 ± 6.7	167~180	162.1 ± 6.3	155~165
Weight, kg	65.2 ± 9.6	59~70	52.1 ± 9.4	48~57
BMI, kg·m-2	22.8 ± 7.1	20~23	19.8 ± 4.1	18.6~21.7

B. Gas System

Gas system is used to measure energy expenditure. The predicted values were compared from indirect calorimeter Cosmed K4b^2 (Cosmed, Srl, Italy). The gas system can realtime monitor VO_2, VCO_2 (Fig. 4.1), and EE (Fig. 4.2). The data can export to Excel form for analysis with AirBeat system. The gas system can be wore by one person for one time. It costs time to guide and help the participants wearing. For one participant, the

whole experiment need around half an hour. And the experiment can not do in anytime of the day. Since it should consider the participants body condition, like no coffee, no smoking, and after meal 2 hours later. Hence, the efficiency is not high.

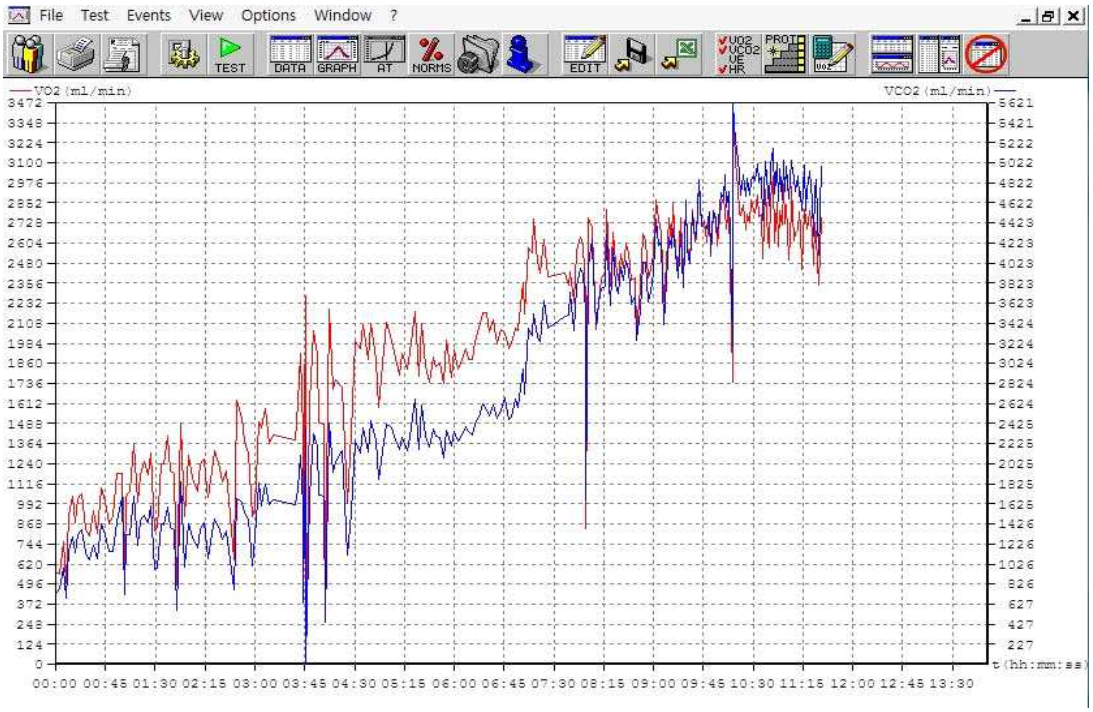

Fig. 4.1 Gas system real-time monitor VO_2 and VCO_2.

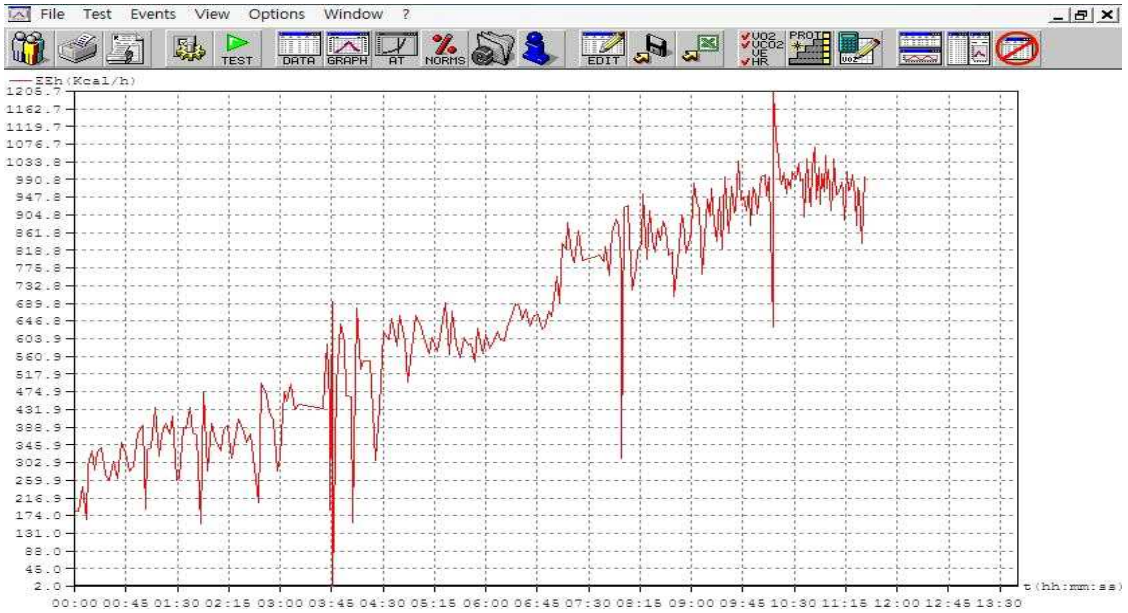

Fig. 4.2 Gas system real-time monitor energy expenditure.

C. Procedure

For determination of the VO_2 / HR regression line, the subjects reported to the laboratory at 3 PM, after lunch at least 2 h later, having avoided substantial physical exercise and smoking that day. VO_2 and HR were recorded during the entire periods (Fig. 4.3): 1: warm-up, 2: five3-min periods of walking or jogging on a treadmill at different speeds, base on Bruce Protocol as in Table 4.2, 3: recovery. The heart rate was recorded with the AirBeat system and O_2-intake was measured using open-circuit system.

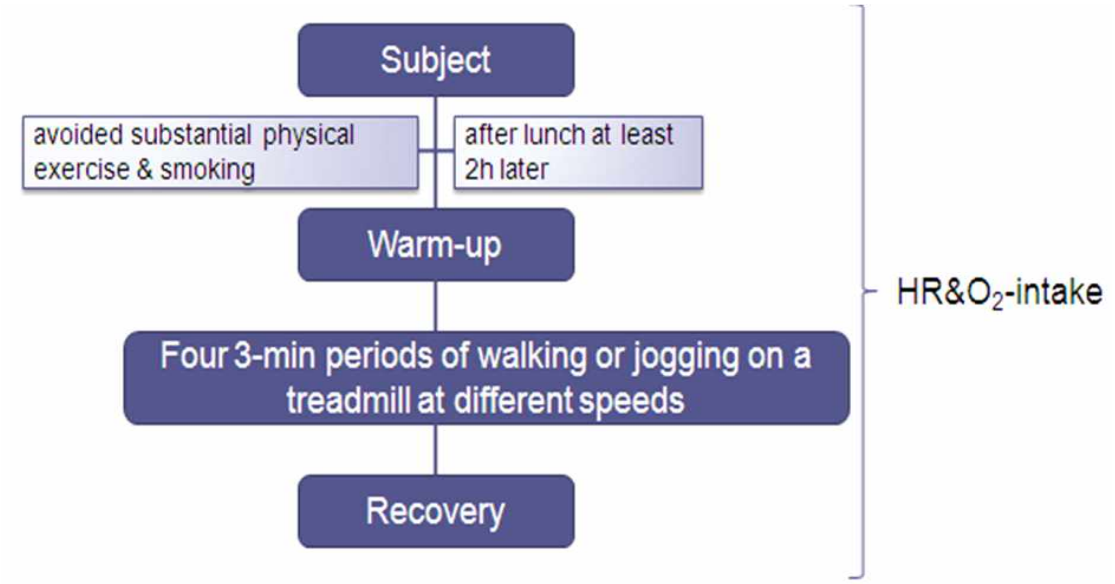

Fig. 4.3 Experiment procedure.

Table 4.2 Participants' activity on treadmill base on Bruce Protocol

Slope (grade)	Speed (km/h)	Time (min)	Stage
10	2.7	3	1
12	4.02	6	2
14	5.47	9	3
16	6.76	12	4

D. Data Analysis

All data were saved in Excel 2003 format. The time were expressed in seconds and beats per min (bpm) for heart rate. Oxygen consumption and carbon dioxide production were expressed in ml per minute (ml/min). Energy expenditure were expressed in Kcal per minute (Kcal/min). All of

the data were a rang in same excel sheet then average each group data. The data can be classified the following groups: Time-HR, Time-VO_2, Time-VCO_2, and Time-EE. These data then were converted to HR-EE, was estimated energy expenditure, then compare with measured the EE (Time-EE)[58].

E. Results

In order to evaluate the function of the incremental RBFN and to realize the final goal under free-living conditions, the design of the experiment was tested in a laboratory and a field test.

1. Laboratory Experiment

The participants were tested on a treadmill using the sub-maximal Bruce protocols in the laboratory, as shown in Fig. 4.4. The treadmill was started at 9.72 $m \cdot s^{-1}$ with a gradient of 10%. The incline of the treadmill was increased by 2% at 3-min intervals. The participants walked and ran until they felt exhausted. For men, the test lasted around 12min, and for women, the test lasted approximately 9~10min. The HR and MI were recorded in real-time by the patch-type sensor, and VO_2 and EE were measured by the gas system.

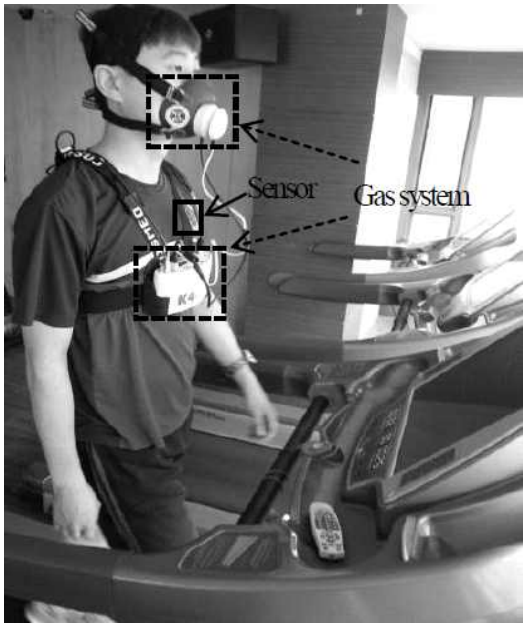

Fig. 4.4. Laboratory experiment on the treadmill.

HR and MI are two major factors for estimate EE. Therefore, they are considered to be two inputs to the incremental RBFN. A total of 76 samples were considered. The number of iterations for all the experiments was ten. 60% of the total data was randomly selected as the training dataset, and the remaining 40% formed the testing dataset. The data were normalized between 0 and 1. The training data were used for the construction of the neuron network, and the testing data were used for the verification of the network. The nonlinear data called “errors” could be calculated by using the root-mean-square error (RMSE) Euclidean value as shown in Equation (4.1).

$$\mathrm{RMSE} = \sqrt{\frac{\sum_{k=1}^{n}\left(EE_k - EE_k^{'}\right)^2}{N}} \qquad (4.1)$$

where N denotes the size of the training or the testing dataset.

The error values were used as the contexts dataset. These contexts were generated using the triangular membership functions that were equally spaced along the domain of an output variable. The membership matrix was initialized with a value between 0 and 1, as shown in Fig. 4.5 (number of contexts: p = 3).

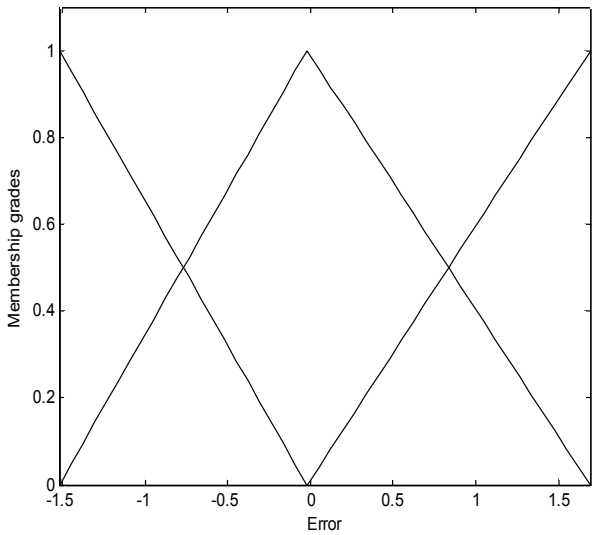

Fig. 4.5. Linguistic contexts produced by the error distribution of treadmill data (p = 3).

The centers could be generated using fuzzy C-means clustering based on each of the contexts. For "p" contexts and "c" centers per context, we obtained c × p clusters. Fig. 4.6 shows the cluster centers generated by using three contexts and three clusters. The cluster centers could be considered the RBFN hidden layer. Therefore, the RBFN model could be constructed as follows: consider two inputs HR and MI to be the input layer, and nine units to be the hidden layer on the basis of the number of contexts and the number of clusters; further, consider the EE to be the output layer.

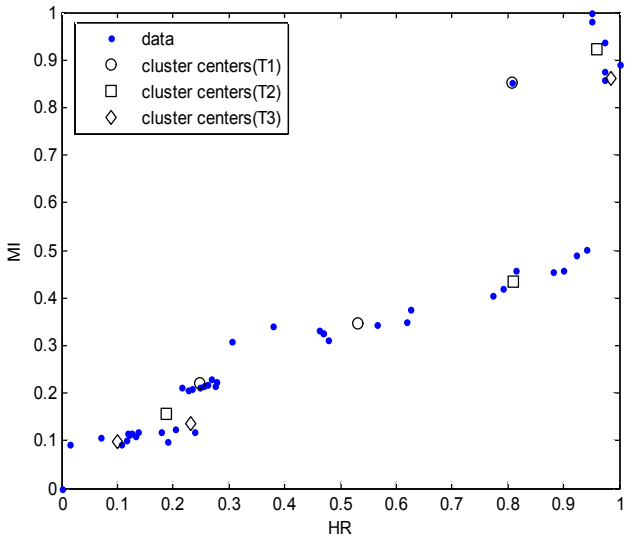

Fig. 4.6. Estimation of cluster centers in each context (p = 3).

The network performance is estimated using the RMSE as the number of contexts and that of clusters increased from three to six and from two to six, respectively. Table 4.3 shows the result of RMSE for the training and the checking datasets. The best-fit model is presented in bold letters (p = 3, c = 3). The comparison of RMSE with previous work is shown in Table 3. The RBFN that we used was a 2-10-1 network with a back propagation algorithm and 1000 epochs with a learning rate of 0.01. The linguistic model (LM) that we used had three contexts and three clusters that were determined by using the trial and error method. The CFCM-RBFN used in the hidden layer increased from 3 to 20 in the experimental design.

Table 4.3 RMSE in incremental RBFN model for training data and testing data.

Treadmill data		Number of contexts (training data)			
		3	4	5	6
No.of clusters per context	2	0.5237	0.5089	0.4798	0.4557
	3	0.4722	0.4436	0.4182	0.3834
	4	0.4367	0.3832	0.3605	0.3276
	5	0.3935	0.3659	0.3050	0.2425
	6	0.3691	0.3245	0.2528	0.1821
Treadmill data		Number of contexts (checking data)			
		3	4	5	6
No.of clusters per context	2	0.6913	0.7506	0.7375	0.7563
	3	0.6627	0.7109	0.7197	0.8622
	4	0.6944	0.7903	0.7819	0.8641
	5	0.7321	0.7162	3.6389	10.938
	6	1.0113	1.1930	99.955	261.54

2. Field Test

The final goal was to realize an accurate estimation of EE under free-living conditions. After the testing in the laboratory environment, all the participants were encouraged to complete four exercise tests in an open field. The first was comfortable walking; the second, jogging; the third, a quick walk; and the last, slow running. Each test course was performed for around 2 min on an oval track. The experiment procedure was designed to progress as naturally as possible. The structure of the

RBFN, as per the laboratory experiment, was used as a reference. The total obtained data in the cases of walking, jogging, a quick walk, and slow running were 157, 60, 63, and 99 sample pairs, respectively. The prediction performance is shown in Fig. 4.7. Table 4.4 lists the RMSE comparison with the LM.

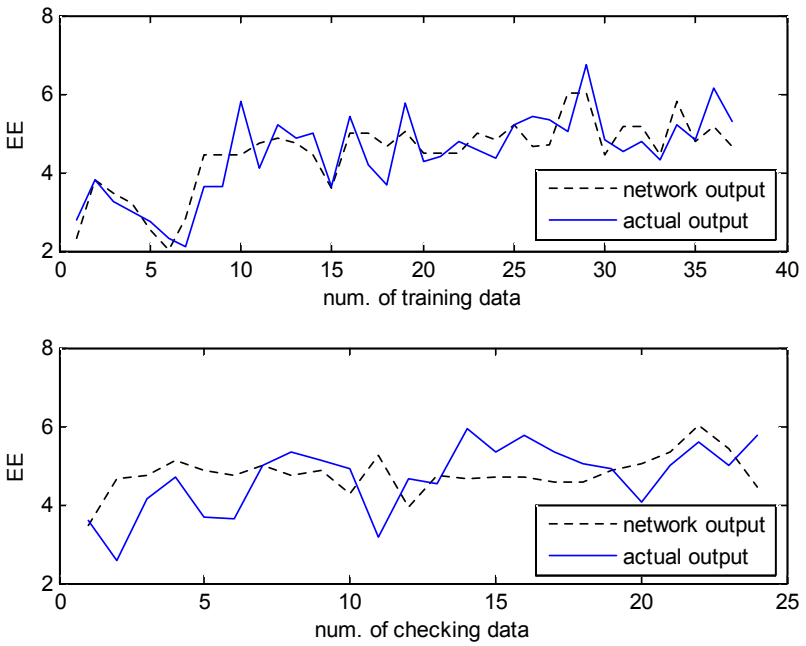

a. Normal walking on school playground.

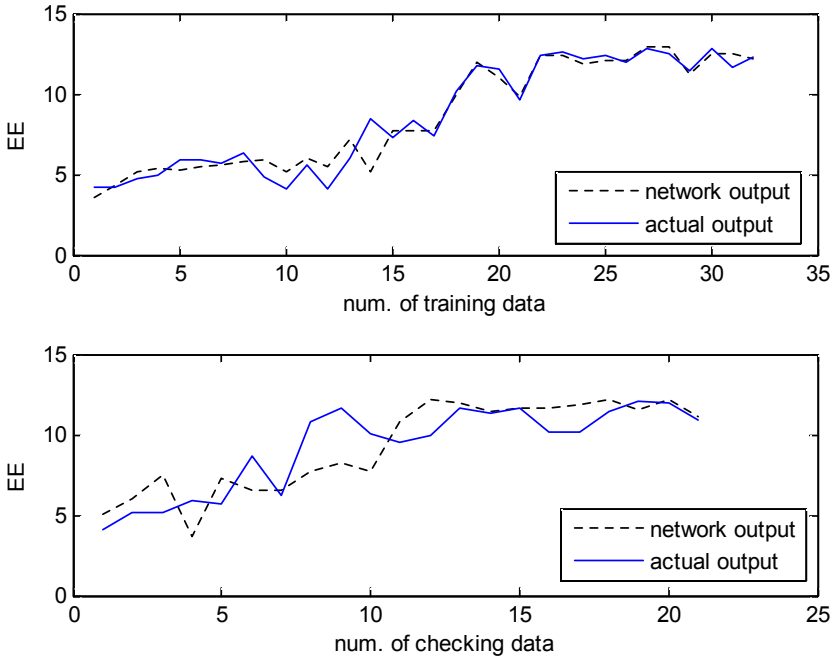

b. Brisk walking on school playground.

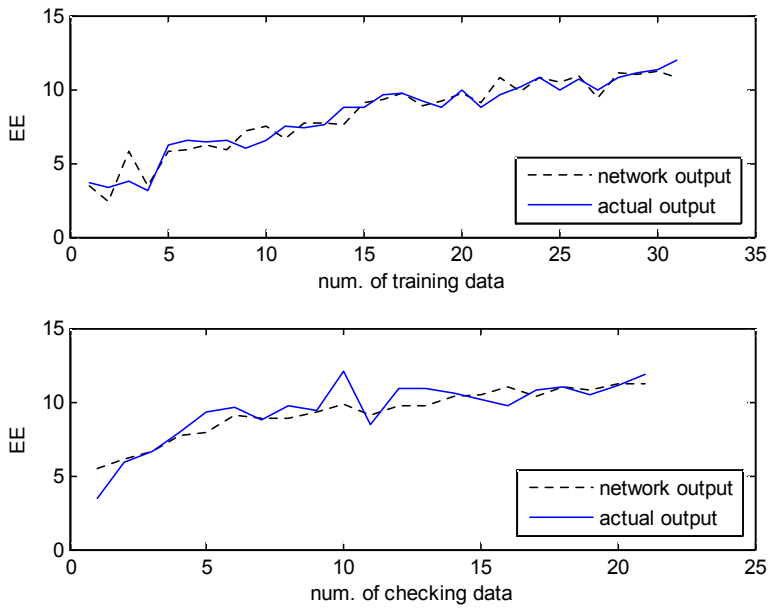

c. Slowest running on school playground.

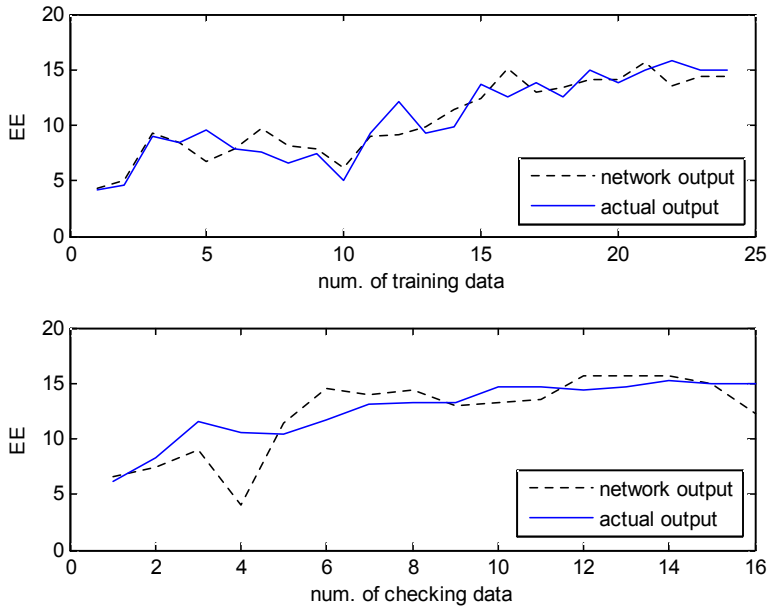

d. Jogging on school playground.

Fig. 4.7. (a-d) EE prediction performance of incremental CFCM-RBFN.

Table 4.4 Comparison of the RMSE values for field exercise data.

Activity	Method	Trn_RMSE	Txt_RMSE
Walking	LM	0.75	1.06
	Incremental CFCM-RBFN	0.60	0.95
Brisk walking	LM	1.47	1.82
	Incremental CFCM-RBFN	0.96	1.68
Slow running	LM	0.79	1.44
	Incremental CFCM-RBFN	0.61	1.07
Jogging	LM	2.0	2.58
	Incremental CFCM-RBFN	1.32	2.45

V. Conclusion

Energy expenditure are used in a variety of applications. The rate of chronic disease such as obesity, hypertension, and diabetic is rapidly increased. Excess nutrient and energy expenditure imbalance are considered major important cause of chronic disease. Energy expenditure is assessed along with energy intake for weight management purpose. The assessment of energy expenditure can play a role in promoting a healthy lifestyle.

Energy expenditure measurements are also important in the study of relationship between physical activity and health. In addition to health promotion and health-related research, energy expenditure measurement can be utilized in fitness and athletic training. Athletes and active sports participants, together with their coaches and personal trainers, can plan their nutrition by utilizing information on expended calories. During fitness training it is often typical to compare energy expenditure values between different exercises, and to select the activities that are perceived most positive and also have relatively high energy expenditure. Coach and athlete can design athlete's daily diet by considering the total energy expended in daily training and living. This is an important issue because a proper nutritional state supports optimal recovery. And body weight and composition can be optimized by utilizing the information on daily energy expenditure.

The method of combine heart rate and motion sensors is most often chosen for assessing physical activity and energy expenditure. We choose this topic because it has many advantages. It overcomes the major weakness associated with HR monitoring or motion sensing alone. For example, HR monitoring is not subject to error in movement sensing such as in detecting the level of activity during resistance exercise, swimming,

and cycling. Likewise, movement sensing complements HR monitoring as it allows differentiation between increased HR caused by physical activity and that caused by non-exercise related influences.

Finally, this study has shown that an incremental CFCM-based RBFN is effective in estimating EE. A significant advantage of this model is that it begins from the LR model and is then refined by adding granular patches, which is considerably different from the preliminary version of the linear model. The other important design element is that the CFCM clustering is applied for calculating the center values, which can reduce the number of iterations, thereby optimizing the network structure. The output space can be optimized by selecting the appropriate number of contexts and the appropriate number of clusters. The experimental results are compared with those of the LM, RBFN, and RBFN-CFCM. This comparison indicates that the sensor module based on the incremental CFCM-based RBFN has the ability to estimate EE during walking and running under both laboratory and free-living conditions (average RMSE = 0.78). Moreover, in a future work, the same approach of incremental modeling could be explored in other domains such as pattern recognition and classification, which could be particularly applied to the field of e-health monitoring.

References

[1] B. E. Ainsworth, W. L. Haskell, A. S. Leon, DR. Jr. Jacobs, H. J. Montoye, J. F. Sallis, and RS. Jr. Paffenbarger, "Compendium of physical activities: classification of energy costs of human physical Activities", Med. Sci. Sports Ex., vol. 25, Jan. 1983.

[2] R. E. Ricklefs, M. Konarzewski, and S. Daan, "The relationship between basal metabolic rate and daily energy expenditure in birds and mammals", Am. Nat., vol. 147, pp. 1047, 1996.

[3] JL. Seale, WV. Rumpler, JM Conway, and CW Miles, "Comparision of doubly labeled water, intake-balance, and direct-and indirect-calorimetry methods for measuring energy expenditure in adult men", Am. J. of Clin. Nutr., vol. 52, pp. 66-71, 1990.

[4] Direct Calorimetry Website, http://sports.jrank.org/pages/7352/direct-calorimetry.html

[5] J. R. S Arch, D. Hislop, S. J. Y., and Wang, International Journal of Obesity, http://www.nature.com/ijo/journal/v30/n9/fig_tab/0803280f1.html

[6] F. Barton and J. F. NuNN, "Totally closed circuit nitrous Oxide/Oxygen anaesthesia", Br. J. Anaesth., vol. 47, pp.350-357, 1975.

[7] Treuth, S., Margarita, A. L. Adolph, and N. F. Butte, "Energy expenditure in children predicted from heart rate and activity calibrated against respiration calorimetry", Am. J. Physiol, vol. 275, pp. E12-E18, 1998.

[8] D. C. Simonson and R. A. DeFronzo, "Indirect calorimetry: methodological and interpretative problems", AJP-Endocrinology and Metabolism, vol. 258, pp. 399-412, 1990.

[9] H. Kumahara, Y. Schutz, and H. Tanaka, "The use of uniaxial

accelerometry for the assessment of physical-activity-related energy expenditure: a validation study against whole-body indirect calorimetry", Br. J. Nutr., vol. 91, pp. 235-243, 2004.

[10] VL. Hood , MH. Granat, DJ. Maxwell, and JP. Hasler, "A new method of using heart rate to represent energy expenditure: The total heart beat index", Arch. Phys. Med. Rehabil., vol. 83, pp. 1266-73, 2002.

[11] R. B. Bradfield, P. B. Huntzicker, and G. J. Fuehan, "Simultaneous comparison of respirometer and heart-rate telemetry techniques as measures of human energy expenditure", Am. J. Clin. Nutr., vol. 22, no. 6, pp. 696-700, 1969.

[12] C. C. Christensen, H. MM. Frey, E. Foenstelien, E. Aadland, and H. E Refsum, "A critical evaluation of energy expenditure estimates based on individual O_2 consumption/heart rate curves and average daily heart rate", Am. J. Clin. Nutr., vol. 37, pp. 464-472, 1983.

[13] GB Spurr, AM Prentice, PR Murgatroyd, GR Goldberg, JC Reina, and NT Christman, "Energy expenditure from minute-by-minute heart-rate recording: comparison with indirect calorimetry", Am. J. Clin. Nutr., vol. 48, pp. 552-529, 1988.

[14] K. L., S. J. Hennings, J. Mitchell, and N. J. Wareham, “Estimating energy expenditure by heart-rate monitoring without individual calibration”, Med. Sci. Sports Exerc., vol. 33, pp. 939-945, 2001.

[15] L. Beghin, T. Bubniok, G. Vaksman, L. Boussard-Delbecque, L. Michaud, D. Turck, and F. Gottrand, "Simplification of the method of assessing daily and nightly energy expenditure in children, using heart rate monitoring calibrated against open circuit indirect calorimetry", Clin. Nutri., vol. 19, no. 6, pp. 425-435, 2000.

[16] S. E. Crouter,, C. Albright, D. R. Bassett, and JR, "Accuracy of Polar S410 heart rate monitor to estimate energy cost of exercise", Med. Sci. Sports Exerc, vol. 36, no. 8, pp. 1433-1439,

2004.

[17] S. J. Strath, D. R. Bassett, JR., A. M. Swartz, and D. L. Thompson, "Simultaneous heart rate-motion sensor technique to estimate energy expenditure", Med. Sci. Sports Exerc., vol. 33, no. 12, pp. 2118-2123, 2001.

[18] A. Wixted, D. Thiel, D. James, A. Hahn, C. Gore, and D. Pyne, "Signal processing for estimating energy expenditure of elite athletes using triaxial accelerometers", IEEE Sens., pp. 798-801, Oct. 2005.

[19] C. B. Liden, M. Wolowicz, J. Stivoric, and A. Teller, "Characterization and implications of the sensors incorporated into the SenseWear armband for energy expenditure and activity detection", Bodymedia Inc. White Papers: 1-7, 2002.

[20] J. M. Jakicic, M. Marcus, K. I. Gallagherm, C. Randall, E. Thomas, F. L. Goss, and R. J. Robertson, "Evaluation of the SenseWear Pro Armband to assess energy expenditure during exercise", Med. Sci. Sports Exerc., vol. 36, no. 5, pp. 897-904, 2004.

[21] C. A. Dorminy, L. Choi, S. A. Akohoue, K. Y. Chen, and M. S. Buchowski, "Validity of a multisensory armband in estimating 24-h energy expenditure in children", Med. Sci. Sports Exerc, vol. 40, no. 4, pp. 699-706, 2008.

[22] Advidsson, D., F. Slindem, S. Larsson, L. Hulthen, "Energy cost in children assessed by multisensory activity monitors", Med. Sci. Sports Exerc, vol. 41, no. 3, pp. 606-611, 2009.

[23] B. Soren, N. Brage, P. W. Franks, U. Ekelund, M. Wong, L. B. Andersen, K. Froberg, and N. J. Wareham, "Branched equation modeling of simultaneous accelerometry and heart rate monitoring improves estimate of directly measured physical activity energy expenditure", J. Appl. Phyiol., vol. 96, pp. 343-351, 2004.

[24] D. R. Bouchardm, and F. Trudeau, "Estimation of energy

expenditure in a work environment: Comparison of accelerometry and oxygen consumption/heart rate regression", Taylor & Francis, vol. 51, no. 5, pp. 663-670, 2008.

[25] S Brage, N Brage, PW Franks, U Ekelund, and NJ Wareham, "Reliability and validity of the combined heart rate and movement sensor Actiheart", Eur. J. Clin. Nutr., vol. 59, pp. 561-570, 2005.

[26] K Rennie, T Rowsell, SA Jebb, D holburn and NJ Wareham. "A combined heart rate and movement sensor: proof of concept and preliminary testing study", Eur. J. Clin. Nutr., vol. 54, pp. 409-414, 2000.

[27] K. Corder, S. Brage, N. J. Wareham, and U. Ekelund, "Comparison of PAEE from combined and separate heart rate and movement models in children", Med. Sci. Sports Exerc., vol. 37, no. 10, pp. 1761-1767, 2005.

[28] B. Dong, S. Biswas, A. Montoye, and K. Pfeiffer, “Comparing metabolic energy expenditure estimation using wearable multi-sensor network and single accelerometer”, Proc. of the IEEE EMBS, pp. 2866-2869, July 2013.

[29] H. Vathsangam, A. Emken, E. T. Schroeder, D. Spruijt-Metz, and G.S. Sukhatme, “An experimental study in determining energy expenditure from treadmill walking using hip-worn inertial sensor”, IEEE Trans. Biomed. Eng., vol. 58, no. 10, pp. 2804-2815, Oct. 2011.

[30] J.S. Wang, C.W. Lin, Y.T. Yang, T.P. Kao, W.H. Wang, and Y.S. Chen, “A pace sensor system with machine learning-based energy expenditure regression algorithm”, Lecture Notes in Computer Science, Springer, vol. 6840, pp. 529-536, 2011.

[31] C.W. Lin, Y.T. Yang, and J.S Wang, “A wearable sensor module with a neural-network-based activity classification algorithm for daily energy expenditure estimation”, IEEE Tans. Inf. Technol. Biomed., vol. 16, no. 5, pp. 991-998, Sept. 2012.

[32] T.C. Wong, J.G. Webster, H.J. Montoye, and R. Washburn, “Portable accelerometer device for measuring human energy expenditure”, IEEE Trans. Biomed. Eng., vol. 28, pp. 467-471, 1981.

[33] A.J. Wixted, D.V. Thiel, A.G. Hahn, C.J. Gore, D.B., Pyne, and D.A. James, “Measurement of energy expenditure of elite athletes using MEM-based triaxial accelerometers”, IEEE Sens. J., vol. 7, pp. 481-488, 2007.

[34] Y.D. Lee, and W.Y. Chung, “Wireless sensor network based wearable smart shirt for ubiquitous health and activity monitoring”, Sens. Actuators B: Chem., vol. 140, pp. 390-395, 2009.

[35] S.M. Powell, and A.V. Rowlands, “Intermonitor variability of the RT3 accelerometer during typical physical activities”, Med. Sci. Sport. Exer., vol. 36, pp. 324-330, 2004.

[36] S.M. Powell, D.I. Jones, and A.V. Rowlands, “Technical variability of the RT3 accelerometer”, Med. Sci. Sport. Exer., vol. 35, pp. 1773-1778, 2003.

[37] E. Ekelund, M. Sjostrom, A. Yngve, E. Poortvliet, A. Nilsson, K. Froberg, N. Wedderkopp, and K.Westerterp, “Physical activity

assessed by activity monitor and doubly labeled water in children", Med. Sci. Sport. Exer., vol. 33, pp. 275-281, 2001.

[38] M. Oliver, G.M. Schofield, H.M. Badland, and J. Shepherd, "Utility of accelerometer thresholds for classifying sitting in office workers", Prev. Med., vol. 51, pp. 357-360, 2010.

[39] F. Xiao, Y.M. Chen, M. Yuchi, and M.Y. Ding, "Heart rate prediction model based on physical activities using evolutionary neural network", In Proc. of the International Conf. on Genetic and Evol. Comp., Shenzhen, China, pp. 198-201, Dec. 13-15, 2010.

[40] F. Xiao, M. Yuchi, M.Y. Ding, J. Jo, and J.W. Kim, "A multi-step heart rate prediction method based on physical activity using Adams-Bashforth technique", In Proc. of IEEE International Symp. on Computational Intelligence in Robotics and Automation, Daejeon, Korea, pp. 355-359, Dec. 15-18, 2009.

[41] M. Yuchi, and J. Jo, "Heart rate prediction based on physical activity using feedforward neural network", In Proc. of Intern. Conf. on Convergence and Hybrid Information Technology, Busan, Korea, pp. 344-350, Nov. 11-13, 2008.

[42] F. Xiao, M. Yuchi, J. Jo, M.Y. Ding, and W.G. Hou, "A research of physical activity's influence on heart rate using feedforward neural network", Springer-Verlag: Berlin/Heidelberg, Germany, vol. 3, pp. 1089-1096, 2009.

[43] H. Vathsangam, A. Emken, E.T. Schroeder, D. Spruijt-Metz, G.S. Sukhatme, "Determining energy expenditure from treadmill walking

using hip-worn inertial sensors: An experimental study", IEEE Trans. Biomed. Eng., vol. 58, pp. 2804-2815, 2011.

[44] C.W. Lin, Y.T.C. Yang, J.S. Wang, and Y.C. Yang, "A wearable sensor module with a neural-network-based activity classification algorithm for daily energy expenditure estimation", IEEE Trans. Inf. Technol. B, vol. 16, pp. 991-998, 2012.

[45] S.S. Kim, and K.C. Kwak, "Development of quantum-based adaptive neuro-fuzzy networks", IEEE Trans. Syst. Man Cy. B, vol. 40, pp. 91-100, 2010.

[46] H. Qu, D. Fang, and H. Xie, "A single-crystal silicon 3-axis CMOS-MEMS accelerometer", IEEE Sens. vol. 2, pp. 661-664, 2004.

[47] J. Lee, and Y. Huang, "ITRI ZBnode: A ZigBee/IEEE 802.15.4 platform for wireless sensor networks", IEEE Conf. on Systems, Man, and Cybernetics, pp. 1462-1467, 2006.

[48] A.T. Purdy, "Developments in non-woven fabrics", Text. Progress vol. 12, pp. 1-86, 1983.

[49] GE Medical System, http://www.egeneralmedical.com.

[50] O. Vainio, and S.J. Ovaska, "Noise reduction in zero crossing detection by predictive digital filtering", IEEE Trans. Ind. Electron, vol. 42, pp. 58-62, 1995.

[51] V.J. Paliczka, A.K. Nichols, and C.A.G. Boreham, "A multistage

shuttle run as a predictor of running performance and maximal oxygen uptake in adults", Br. J. Sports Med., vol. 21, pp. 163-165, 1987.

[52] W. Poltorak, "The significance of environmental factors for physical development of adolescents", Hum. Movement, vol. 10, pp. 35-45, 2009.

[53] R.R. Vickers, J.H. Reynolds, J.R. Jordan, and L.K. Hervig, "An evaluation of a combat conditioning trial program", Technical Report, 09-02, 2008.

[54] R. Bruce, "Method of exercise testing step test, bicycle, treadmill, isometrics", Am. J. Cardiol., vol. 33, pp. 715-720, 1974.

[55] J. S. R. Jang, C.T. Sun, and E. Mizutani, "Neuro-Fuzzy and soft computing", Prentice Hall, pp. 238-246, 1997.

[56] X. Hong, "A fast identification algorithm for Box-Cox transformation based redial basis function neural network", IEEE Trans. Neural Netw., vol. 17, no. 4, pp. 1064-1069, July 2006.

[57] S. Ferrari, M. Maggioni, and N. A. Borghese, "Multiscale Approximation with hierarchical radial basis functions networks", IEEE Trans. Neural Netw., vol. 15, no.1, pp. 178-188, Jan. 2004.

[58] M. Li, K. H. Byun, H. J. Kim and Youn Tae Kim, "Patch type sensor module for estimating the energy expenditure", Proc. of IEEE Sensors, pp. 1445-1458, 2009.

List of Publications

1. Journal paper

1) **Li Meina** and Youn Tae Kim, "Development of Patch-Type Sensor Module for Real-Time Monitoring of Heart Rate and Agility Index Design", Sensor and Actuator A, vol. 173, pp. 277-283.

2) **Li Meina**, Keun Chang Kwak, and Youn Tae Kim, “Intelligent Predictor of Energy Expenditure with the Use of Patch-Type Sensor Module”, Sensors, vol. 12, pp. 14382-14396.

2. Conference paper

1) **Li Meina**, Kyeong Ho Byun, Hyo Jung Kim, Jaemin Kang, and Youn Tae Kim, "Patch Type Sensor Module for Estimating the Energy Expenditure", International Conference on IEEE Sensors, New Zealand, pp. 1455-1458, Nov. 2009.
2) **Li Meina**, Dinh Luan, Ji Hwan Lee, and Youn Tae Kim, "In-situ Monitoring of Energy Expenditure by the Application of Wireless Patch Type Sensor Module", AMA-IEEE Medical Technology International Conference on Individualized Healthcare, Washington. DC, USA, pp. 32, Mar. 2010.
3) Dinh Luan, **Li Meina**, Ji Hwan Lee, and Youn Tae Kim, "Algorithm for Real-Time Wireless Monitoring of Heart Rate and Agility Index", AMA-IEEE Medical Technology International Conference on

Individualized Healthcare", Washington. DC, USA, Mar. 2010.

4) **Li Meina**, Jang Myoung Kim, and Youn Tae Kim, "A Combined Heart Rate and Agility Index Sensor for Estimating the Energy Expenditure", International Conference of IEEE Sensors, Hawaii, USA, vol. 43, pp. 809-812, May. 2010.

5) Kyeung Ho Kang, **Li Meina**, Wang Keun Oh, and Youn Tae Kim, "A Portable System for Measuring Energy Expenditure in Free-Living Adults", AMA-IEEE Medical Technology Conference, USA, 2011.

6) **Li Meina**, Kyeung Ho Kang, Wang Keun Oh, and Youn Tae Kim, "Monitoring Energy Cost Using a Wireless Patch Type Sensor Module with Embedded Algorithm", IEEE Sensor Application Symposium, Italy, 2012.

Acknowledgement

First and foremost, I would like to express my sincere gratitude to my supervisor, Professor Youn Tae Kim for his supervision, understanding, support, encouragement and personal guidance for the present thesis. I am deeply grateful to all of the professors from whom I have learnt great deal of knowledge.

Beside, my deepest appreciation to committee members, Prof. Sung Bum Pan, Dr. Myung Ae Chung, Prof. Keun Chang Kwak, and Prof. Soon Soo Oh, for their detail review, constructive criticism and excellent advice during the preparation of this thesis.

During this work I have collaborated with all my lab mates for whom I have great regard, and I wish to extend my warmest thanks to all those who have helped me with my work in the Department of IT Fusion Technology.

Finally, my deepest gratitude to my family in supporting me. I owe my loving thanks to my mother for her love, understandings and encouragement in every moment of my life. 我要谢谢一直以来支持我的妈妈，和关心我爱护我的家人，谢谢！

The financial support of Prof. Youn Tae Kim and the University of Chosun is gratefully acknowledged.